BMC Infectious Diseases

RESEARCH

Open Access

Virtual screening assisted identification of a phytocompound as potent inhibitor against *Candida lusitaniae*; an *in-silico* study

Rimsha Timotheous[1], Habiba Naz[1], Usman Arif[2], Momna Toqeer Dar[1], Muhammad Farhan Sarwar[1*], Mudassar Fareed Awan[1], Sajed Ali[1] and Safia Obaidur Rab[3]

Abstract

Candida lusitaniae is one of the fungal species which causes serious health illnesses including peritonitis, vaginitis and fungemia, among others. Several antifungal drugs have been designed to tackle its infections but their efficacy is still questionable due to their associated side effects. Hence, there is a need to design those drugs which possess comparatively higher degree of therapeutic potential. Phytochemicals were selected in this regard because these compounds which satisfactorily follow this criteria as, their therapeutic index is comparatively larger than the synthetic drugs. Considering this fact, different phyto-compounds were opted in this research work to estimate their therapeutic efficiency against the secreted aspartyl proteinase (SAP) of *C. lusitaniae* since, it assists this pathogen in developing the infections. Initially, the structure of SAP was modelled for subsequent docking analysis. The results of molecular docking suggested that three compounds, opelconazole, daidzin 4'0-glucuronide and naringin exhibited better docking scores. Afterwards, ADME analysis of all these four compounds was performed to comprehend their drug-likeness attributes. The results of ADME analysis revealed that only the daidzin 4'0-glucuronide followed all the required parameters. Lastly, MD simulations were conducted in which top three compounds in context of docking scores along three approved anti-fungal drugs in complex with SAP were incorporated for the comparative analysis. The overall results of MD simulations suggested that daidzin 4'0-glucuronide exhibited comparatively better results. This outcome indicated that this particular compound not only showed better binding affinity with SAP during docking analysis and fulfilled all of the drug-likeness moieties among other compounds but also, displayed better simulation results, leading to a conclusion that daidzin 4'0-glucuronide could be a potential drug candidate against *C. lusitaniae*. However, its real-time efficacy could only be validated in clinical settings.

Keywords *C. lusitaniae*, Molecular docking analysis, Phytochemicals, Secreted aspartyl proteinase (SAP), Virtual screening

Introduction

First documented as a human pathogen in 1979, *Candida lusitaniae (C. lusitaniae)* has been implicated in a multitude of afflictions, including fungemia, peritonitis, and additional infections, primarily affecting patients suffering from underlying malignancies, those subjected to chemotherapy, and individuals harboring intravenous catheters or those, exposed to broad-spectrum antibiotics [1]. Responsible for roughly 19.3% of fungemia cases

*Correspondence:
Muhammad Farhan Sarwar
mf.sarwar13@gmail.com
[1] Department of Biotechnology, Knowledge Unit of Science (KUSC), University of Management and Technology (UMT) Sialkot Campus, Sialkot, Pakistan
[2] Centre of Excellence in Molecular Biology, University of the Punjab, Lahore, Pakistan
[3] Department of Clinical Laboratory Sciences, College of Applied Medical Science, King Khalid University, Abha, Saudi Arabia

[2] and approximately 1.7% of all genitourinary candidiasis incidents in ambulatory patients, *C. lusitaniae* poses a notable threat to public health [3]. Associated with elevated mortality rates originating from its inherent resistance to conventional antifungal medications, such as amphotericin B, 5-fluorocytosine, and fluconazole, *C. lusitaniae* has historically led to severe fatalities prior to the introduction of fluconazole therapy. Nonetheless, contemporary mortality rates seldom surpass 5%, reflecting improvements in treatment efficacy [4]. Notwithstanding the advancements, the prevalence of *C. lusitaniae* infections continues to increase, presenting a frightening challenge amidst the growing population of immune-compromised individuals [5, 6].

C. lusitaniae, possesses various virulence factors that contribute to its pathogenicity. These factors include cell wall barriers, adherence mechanisms, dimorphism, biofilm formation and stress-tolerant proteins [7]. Among these factors, there are also the hydrolytic enzymes which play a crucial role in the pathogen's ability to invade the host and evade its immune response [8]. One of the key hydrolytic enzymes produced by *C. lusitaniae* is the Secreted Aspartyl Proteinase (SAP). The SAP is one of the critical virulence factors as it facilitates tissue invasion by degrading host proteins and also, by disrupting the defense mechanisms. The ability of SAP to degrade a variety of proteins allows the pathogen to thrive in different host environments and contributes significantly to its pathogenicity [9]. Due to all such significant attributes especially, in assisting the virulence of the pathogen, the SAP of *C. lusitaniae* which is also known as candidapepsin protein, was majorly targeted for the current research work.

As far as the current treatment methods to treat *C. lusitaniae* infections particularly by using the antifungal drugs including Fosmanogepix [10] (Approved in 2022), Opelconazole and Olorofim [11] (Approved in 2023) is concerned, their efficacy is uncertain due to their associated side effects in patients. Some of the common side effects include vomiting, abdominal pain, dizziness,, and diarrhea [12–14]. Therefore, in response to the urgent need for alternative therapeutic sources, the adoption of unconventional treatments has gained significance. One promising avenue is the utilization of phytochemicals, as potential therapeutic agents [15]. Plant compounds, known for their diverse biological activities and health benefits, offer a natural and potentially safer alternative to synthetic chemical drugs due to no fungal resistance against them [16, 17], they are less likely to cause severe adverse effects or toxicity [18]. These compounds can often be obtained from dietary sources or herbal supplements, making them easier to incorporate into treatment regimens [15]. Moreover, their diverse pharmacological effects make them plausible candidates for therapeutic interventions.

Therefore, the selection of 35 phytochemicals was made based on the basis of specific parameters such as antimicrobial effectiveness and drug likeness characteristics. These parameters were crucial in determining the potency and effectiveness of these compounds in inhibiting certain biological targets. The overall methodology for this study involved retrieving the amino acid sequence of the SAP from UniProt (https://www.uniprot.org/), followed by predicting its three dimensional (3D) model by employing the trRosetta server (https://yanglab.qd.sdu.edu.cn/trRosetta/). Afterwards, the predicted structure was stereochemically evaluated through Ramachandran plot. This prediction of the protein model and its evaluation was primarily performed to subject it to the molecular docking analysis in which the targeted ligands were screened out based upon the docking energy scores. The selected compounds were then proceeded for subsequent ADME analysis for further screening and selection of a potent drug candidate. The final results suggested that *daidzin 4'-0-glucuronide* fulfilled the required pharmacokinetic characteristics. Consequently, the molecular dynamics simulations were conducted using Desmond, to assess the structural stability flexibility, protein–ligand interactions and the calculations of binding free energies through MMGBSA, during the 200 ns simulations of the docked complexes. This particular analysis presented favorable results indicating that the docked complex (SAP-daidzin 4'-0-glucuronide) under study was stable enough upon simulations.

Methods

Amino acid sequence retrieval

Putative Secreted Aspartyl Proteinase (SAP) or candidapepsin protein was the targeted protein of this study. In order to perform the subsequent analyses, its amino acid sequence was required. Hence, it was retrieved from UniProt (UniParc accession ID: UPI0012A87966) (https://www.uniprot.org/) which is a free source and comprehensive database that provides free and easy excess to a wide range of protein sequence and functional information [19]. While, the amino acid sequence length of the protein under study was 396.

Structural modeling of target protein

The retrieved amino acid sequence was then subjected to modelling to predict the three dimensional (3D) model. For this purpose, the trRosetta online server (https://yanglab.qd.sdu.edu.cn/trRosetta/#:~:text=trRosetta%20is%20an%20algorithm%20for,by%20a%20deep%20neural%20network.) was employed [20]. The trRosetta, is a sophisticated tool designed for predicting protein

structures. It also possesses the capability to perform de novo modeling, allowing it to construct protein structures without solely relying on pre-existing templates. This aspect is particularly valuable for proteins with unique sequences or those lacking well-defined experimental structures. Additionally, trRosetta excels in automatically identifying homologous templates by seamlessly integrating de novo modeling with template-based modeling (TBM). By using this hybrid approach, trRosetta can efficiently generate initial models based on structurally similar sequences found in public databases. This combination of de novo and template-based strategies empowers trRosetta to deliver accurate and reliable 3D models across a diverse spectrum of protein targets, showcasing its versatility and effectiveness in protein structure prediction tasks. In the current perspective, it employed different protein models from protein data bank (.pdb) to predict the 3D structure of SAP while, the FASTA format amino acid sequence of the respective protein was given as input to be processed for modelling [21]. Whereas, different parameters were taken into consideration to select the appropriate protein model including the confidence score which exhibits the alignment between the query and the template sequence. This score also refers to the scope of the query sequence that gets aligned with the sequence of the template. Additionally, the sequence identity score which indicates the extent of amino acids in the aligned regions between the query and the template sequences, is also highly significant while inferring the required parameters. Furthermore, the E-value (expected value) is also one of the important factors of this server which shows, either the alignment between the query and the template is due to chance or not. Afterwards, the Z-score refers to calculate the statistical significance of the match which is discussed in context of E-value. The better the match, the higher will be the Z-score and ultimately the significance will also be the more. Normally, a Z-score higher than 10 is regarded very significant which signifies the reliability and ensures the precision of the modelled protein structure.

Stereo-chemical evaluation of predicted structure

The predicted structure of the protein was then analyzed by incorporating the PROCHECK server (https://saves.mbi.ucla.edu/) [22]. PROCHECK generates Ramachandran plot which is basically graphical representation of the torsion angles phi (?) and psi (?) of the amino acid residues in a protein structure. The graph is divided into four quadrants, showing different regions including allowed (most favorable), disallowed (not-favorable) and additionally allowed regions. These regions are represented with different colors as red color corresponds to the allowed region, yellow to the additionally allowed and white color indicate the disallowed region. The allowed region represents the energetically favorable conformations of the protein residues that are not sterically hindered while the dis-allowed region represents those conformations of the protein residues that are sterically hindered having least permitted rotations which are energetically unfavorable [23]. This also assist to identify the potential errors presents in the backbone conformation of the given protein. Ramachandran plot presents the relevant results as Ramachandran score where the higher scores indicate the better quality of the protein model.

Molecular docking analysis

To conduct the molecular docking analysis in this study, the Molecular Operating Environment (MOE) *version 2015* was employed. MOE is a powerful computational platform, equipped with advanced algorithms and capabilities suitable for carrying out molecular docking simulations. Prior to executing the molecular docking analysis, several preliminary preparations were undertaken to ensure accurate and reliable results. Firstly, the receptor protein and the library of ligands were prepared. Secondly, an appropriate model was implemented for the docking process. Thirdly, a specified scoring method was chosen to estimate the binding affinities of the docked complexes. Lastly, the number of poses considered for each ligand during the docking analysis was also set to a certain number. Once these preparations were completed, MOE was configured to execute the molecular docking analysis. MOE's robust algorithmic framework, coupled with its intuitive interface, streamlined the execution of the docking simulations, thereby accelerating the progression towards the identification of novel lead compounds. Throughout the course of this study, MOE served as a versatile and indispensable tool for conducting molecular docking analyses, guiding the selection of promising ligands and shedding light onto the interaction mechanisms between the receptor protein and the library of 35 ligands.

Energy minimization and preparation of the receptor protein

To obtain an optimized conformation of the receptor protein, the initial stage involved was performing the energy minimization by utilizing MOE's built-in energy minimization tool. Energy minimization is a technique aimed at reducing the overall potential energy of a molecular system, thereby improving its stability and accuracy. By employing this approach, the receptor protein's structure became less strained and more realistic, better approximating its native state. Following the completion of energy minimization, another crucial step was carried out within the MOE environment, adding polar

hydrogen atoms. This procedure ensures that the receptor protein's interactions with ligands would represent accurately, leading to more reliable docking simulations and subsequent analysis. Both energy minimization and polar hydrogen atoms' addition were the integral components of preparing receptor proteins for downstream computational investigations, such as molecular docking and virtual screening. These preparatory steps improve the quality of the input structures, thereby increasing the reliability and validity of the results obtained from these techniques [24]. Afterwards, the active site of the receptor protein was determined by employing the 'site-finder' tool of MOE. Resultantly, several sites were predicted while, the largest among all of them were opted which was consisted of 85 residues. This selection was made for providing an adequate area to the interacting ligands so that they could bind with the residues of the binding site in their most appropriate pose and orientation, leading to the formation of a stable docked complex.

Preparation of the ligands library

To execute molecular docking analyses, a collection of 38 ligand molecules was assembled. Out of total 38, there were 35 phytochemicals that were selected on the basis of their antimicrobial and specifically, their antifungal properties while, the rest of 3 compounds were the approved anti-fungal drugs which were included as control. As far as the selection of the phytochemicals is concerned, various studies have reported their not only the antimicrobial attributes but the anti-fungal characteristics as well [25–27]. The phytochemicals were retrieved from the expansive catalog offered by the ChEBI (Chemical Entities of Biological Interest) database (https://www.ebi.ac.uk/ChEBI/) [28], which is a renowned open-access repository dedicated to small chemical compounds of biological importance. ChEBI supplies a lot of detailed information about each compound, comprising chemical structures, nomenclature, synonyms, and additional properties [29]. Whereas, the control drugs were retrieved from PubChem database (https://pubchem.ncbi.nlm.nih.gov/) since, they were not available on ChEBI. To prepare the library of 38 ligands, the corresponding chemical structures were downloaded from ChEBI and PubChem in structured data file (*.sdf*) format. The*.sdf* file is a commonly accepted format for storing chemical information, containing details such as molecular connectivity, atomic coordinates, and elemental compositions. Utilizing SDF files also ensures the compatibility with various computational tools, including molecular docking engines. The preparation of this library followed a virtual screening strategy, aiming to identify promising phytochemicals/compounds capable of interacting favorably with the target receptor protein. All of the selected phytochemicals along the control drugs for this particular study are presented in the Table 1 which is comprised of their names, ChEBI/PubChem ID's, molecular structures and natural sources.

Execution of molecular docking

Following the preparation of the receptor protein and the library of 35 ligands, several crucial parameters were incorporated to carry out the molecular docking analysis. One of the most notable selections included implementing the Induced Fit Refinement (IFR) model for this study. IFR enables structural flexibility during the docking process, thereby promoting the generation of docked complexes featuring optimal orientations and significant docking energies. Adopting the IFR model allowed the receptor protein to adapt its structure upon ligand binding, mimicking the conformational changes that occur naturally when a ligand interacts with its target. Consequently, the resulting docked complexes exhibited greater fidelity compared to rigid docking methods, wherein the receptor protein remains static throughout the entire simulation. Additionally, the London dG scoring method was chosen to calculate the scores of the docking parameters. The London dG score estimates the binding affinity of a ligand-receptor complex, taking into account van der Waals forces and electrostatic interactions. This scoring function enabled the ranking of the docked complexes based on their estimated binding affinities, thus facilitating the identification of the most promising ligands. Lastly, the number of poses considered for each ligand during the docking analysis was set to more than 1. Generating multiple poses per ligand increased the likelihood of identifying low-energy binding modes, therefore, enhancing the confidence in the required results of the molecular docking analysis. Overall, incorporating the IFR model, London dG scoring method, and considering multiple poses per ligand, contributed significantly to the molecular docking analysis in yielding insights into the interaction mechanisms between the receptor protein and the selected ligands.

Selection of the potential ligands/compounds

After the docking analysis, some ligands were shortlisted on the basis of their molecular docking scores. We had set a threshold value of -7 kcal/mol to screen out the potentially docked compounds. In this way, only the ligands which exhibited the docking energy scores less than -7 kcal/mol were opted for the subsequent and final scrutiny through the ADME analysis. For this purpose, the R language assisted scatter plot was constructed. Various libraries of R was utilized in this context including the *read.xlsx* and *ggplot2*. This particular analysis made

Table 1 The details of selected phytochemicals along the control/approved drugs for this research work including their names, ChEBI ID, molecular structures and natural sources

Sr. no.	Names of phytochemicals	ChEBI ID's	Molecular Structures	Natural Sources
1	(+)-Epicatechin	CHEBI: 90		*Theobroma cacao* (cocoa beans)
2	Baicalin	CHEBI: 2991		*Scutellaria baicalensis* (Chinese skullcap) roots
3	Chlorogenic	CHEBI: 3635		*Cynara* spp. (artichoke tree)
4	Chrysin 5,7-dimethyl ether	CHEBI: 3694		*Passiflora incarnata* (passionflower)
5	Curcumin	CHEBI: 3962		*Curcuma longa* (turmeric) rhizome
6	(+)-Epigallocatechin 3-gallate	CHEBI: 4806		*Camellia sinensis* (Green tea leaves)
7	Galangin	CHEBI: 5292		*Alpinia officinarum* (galangal) root
8	Isorhamnetin	CHEBI: 6052		*Ginkgo biloba* (Gingko)
9	Melvidin	CHEBI: 6674		*Vaccinium myrtillus* (bilberry)
10	Nobiletin	CHEBI: 7642		*Citrus depressa, Citrus reticulata* (citrus peels)
11	Sinensetin	CHEBI: 9318		*Citrus sinensis* (sweet orange) peel
12	Tangeretin	CHEBI: 9469		*Citrus reticulata* (Tangerine peel)
13	5,7-dihydroxy-4-methylflavone	CHEBI: 15335		*Artemisia annua* (sweet wormwood)
14	(+)-Catechin	CHEBI: 15698		*Camellia sinensis* (tea leaves)
15	Luteolin	CHEBI: 15864		*Taraxacum officinale* (dandelion)
16	Quercetin	CHEBI: 16243		*Allium cepa* (onion)
17	Syringetin	CHEBI: 18398		*Mucuna pruriens* (velvet bean)
18	Pelargonidin	CHEBI: 28069		*Fragaria* spp. (Strawberries)
19	Genistein	CHEBI:28698		*Glycine max* (Soybeans)
20	Delphinidin	CHEBI: 28438		*Vaccinium myrtillus* (bilberry)
21	Hesperidin	CHEBI: 28775		*Citrus reticulata* (mandarin orange)
22	Naringin	CHEBI: 28919		*Citrus paradisi* (grapefruit)
23	Daidzin; 7-o-beta-D-glucoside	CHEBI: 42561		*Glycine max* (Soybeans)
24	Fisetin	CHEBI: 42585		*Rhus succedanea* (wax tree)
25	Naringenin	CHEBI: 50282		*Citrus paradisi* (grapefruit)
26	Doxycycline	CHEBI: 50683		Tetracycline
27	Myricetin(-)	CHEBI: 50799		*Myrica rubra* (bayberry)
28	Kaempferol-sinonidin	CHEBI: 50873		*Ginkgo biloba* (Gingko)
29	Nordopetidin	CHEBI: 50916		*Citrus aurantium* (bitter orange)
30	(+)-Epicatechin -3,5,7,3',4'-pentol	CHEBI: 70235		*Camellia sinensis* (Green tea leaves)
31	(+)-Gallocatechin	CHEBI: 71225		*Camellia sinensis* (Green tea leaves)
32	Cyanidin(1+)	CHEBI: 71692		*Vaccinium myrtillus* (bilberry)
33	Peonidin	CHEBI: 75114		*Vaccinium myrtillus* (bilberry)
34	Petunidin	CHEBI: 75116		*Vaccinium myrtillus* (bilberry)
35	Daidzin 4'-O-glucuronide	CMDB: 134725		*Glycine max* (Soybeans)
36	3-O-caffeoylquinic acid	CHEBI: 64413 80		Chicory (*Cichorium intybus*)
37	Apigenin	CHEBI: 18346		Celery (*Apium graveolens*)
38	Biochanin A	CHEBI: 17793		Soybean (*Glycine max*)
39	Pinocembrin	CHEBI: 28043		Scots Pine (*Pinus sylvestris*)
40	Emodin	CHEBI: 42223		Rhubarb (*Rheum palmatum*)
41	Physcione	CHEBI: 66705		no
42	Formononetin	CHEBI: 18098		Red Clover (*Trifolium pratense*)
43	Galangin	CHEBI: 5292		Galangal (*Alpinia officinarum*)
44	Glycitein	CHEBI: 34778		Soybeans (*Glycine max*)
45	Homoeriodictyol	CHEBI: 74998		Citrus fruits
46	Liquiritinoside B	CMDB: 176253		Licorice (*Glycyrrhiza glabra*)
47	Liquiritinoside F	CMDB: 44030 157		Licorice (*Glycyrrhiza glabra*)
48	Maritc	CHEBI: 75992		Guava (*Psidium guajava*)
49	Oroxylin A	CHEBI: 81068		Huxul Skullcap (*Scutellaria baicalensis*)
50	Pinocembrin	CHEBI: 28157		Fingerroot (*Boesenbergia pandurata*)
51	Rosmarinic acid	CHEBI: 17228		Rosemary (*Salvia rosmarinus*)
52	Rutin	CHEBI: 28527		Buckwheat (*Fagopyrum esculentum*)
53	Scutellarein	CHEBI: 9901		Skullcap (*Scutellaria lateriflora*)
54	Tectochrin	CHEBI: 30545		Siberian Lunch (*Lunis sibirica*)
55	Wogonin	CHEBI:18643		Andrographis (*Andrographis paniculata*)
Control Drugs (Approved anti-fungal drugs)				
56	Fosmanogepix	44127754		*Approved anti-fungal*
57	Opelconazole	121303526		*Approved anti-fungal*
58	Olorofim	91885968		*Approved anti-fungal*

the screening and selection process of the best docked compounds more precise and accurate.

ADME analysis

In addition to the docking energy scores based short-listing of the potent ligands, the pharmacokinetics/ADME analysis of the screened-out compounds were performed for final selection. This particular analysis was performed by incorporating the SwissADME online tool (http://www.swissadme.ch/) [30]. This web-based platform offers a comprehensive suite of features that facilitate the analysis of absorption, distribution, metabolism, and excretion (ADME) parameters, along with other pharmacokinetic properties of any compound under study. It gives a free access to a wide range of fast as well as robust predictive models to compute all these parameters, including in-house proficient methods like BOILED-Egg, iLOGP and bioavailability radar [31]. Additionally, SwissADME allows for the computation of physicochemical descriptors and medicinal chemistry attributes which are essential for understanding the compound's behavior in biological systems [32]. This online tool improves the efficiency and accuracy of predicting the important pharmacokinetic properties. In this way, it helps the researchers to make conclusive decisions and improve the develop optimization strategies in the context of drug development.

LigPlot analysis

LigPlot is a program that is used to generate a schematic diagram to elaborately showcasing the protein-ligand interactions [33]. A 2D representation, known as ligand plot, is generated to provide a simple and informative visualization of the intermolecular interactions and their strengths including hydrogen bonds, hydrophobic interactions and atom accessibilities. This plot also enables a comprehensive data about the affinity and binding of the ligand. In the current perspective, it provided significant insights regarding the final docked complex to highlight certain amino acids in the receptor protein which interacted with the potential ligand. These amino acids were labeled and colored differently depending on the type or strength of the interactions, they were involved in [34].

Molecular dynamics (MD) simulations

For molecular dynamics simulations, the Desmond software was incorporated. It is a high-performing graphics processing unit (GPU) assisted simulation suite for simulating biological systems including macromolecules and their complexes. In the current study, the docked complexes were solvated in a suitable solvent model, typically TIP3P water, within a periodic boundary box (12 Å) to mimic a physiological environment. Counter ions were

added to neutralize the overall charge of the systems, ensuring that the simulations could be performed under conditions that closely resemble a natural biological environment. For this, the 68 sodium (Na +) ions with a concentration of 77.056 mM and 45 chloride (Cl-) ions were added to the system with a concentration of 50.993 mM. The sodium ions provided a total positive charge of + 68, while the chloride ions provided a total negative charge of -45. This balance was highly essential for maintaining the electrostatic stability of the overall system during the simulations. While, the Optimized Potentials for Liquid Simulations—All Atom (OPLS-AA) force-field was applied to both the protein–ligand complex and the apo protein to calculate the interactions and forces within the systems accurately. The systems were set to run under physiological conditions, with a temperature of 300 K and pressure of 1 atm. A time step of 2 femtoseconds (fs) was used to ensure numerical stability. Initially, the simulations were run for 100 ns, but during the last 50 ns the apo protein was showing a bit unstable behavior. Hence, the extended simulations were then run of which the time duration was set to 200 ns, during which the dynamic behavior of the system was recorded. During this particular time period, the stability of the protein was ensured and then its last frame was extracted since, it was showing the most stable conformation, for another round of docking simulations to produce comparatively stable complexes. Afterwards, by following the same protocol, two rounds of the MD simulations were finally run for 200 ns and the dynamic behavior of the systems was again recorded for each of the complex. In this first round, the RSMD and RMSF of daidzin 4'0-glucuronide was analyzed in comparison with hesperidin and naringin. After that, during the second run, daidzin 4'0-glucuronide was comparatively assessed by involving the reference drugs. In both of these contexts, the docked complexes were subjected in the simultaneous simulations for both of the time. The systems underwent energy minimization to remove any steric clashes and relax the structures. Following this, the systems were gradually heated from 100 to 300 K, and equilibrated under constant temperature and pressure (NPT ensemble) for a sufficient duration to stabilize density and temperature distribution. The production MD simulations the docked complexes were carried out for 200 ns. Trajectory data were recorded at regular intervals to analyze the stability and dynamic behavior of the protein-ligand complex, compared to the apo protein. After the MD simulations, the Maestro, which is the intuitive graphical interface of the Schrodinger software suite was utilized for further interactions and interpretations of results. From Maestro, various graphs such as protein-ligand RMSD, protein RMSF, ligand RMSF, protein-ligand contacts, etc., were obtained, aiding in the comprehensive analysis of molecular dynamics simulations and protein-ligand interactions in the current study.

Molecular mechanics generalized born surface area (MM-GBSA) binding energies calculations

To calculate MM-GBSA binding energies using Desmond software, the protein-ligand complex was first prepared by removing water molecules and the structures were optimized. Subsequently, the overall system was relaxed as a result of simulations and the binding energies were computed. Snapshots were extracted from the trajectory, and for each snapshot, the MM-GBSA binding energy was calculated. These energies were analyzed to comprehend the interactions between the protein and ligand. Afterwards, a comprehensive report was compiled regarding the computed MM-GBSA binding energies to infer the overall results. The results were summarized in a table at the end of the report, providing a clear overview of the binding energies for the complex.

The overall research methodology followed in this study is illustrated in the Fig. 1.

Results

Targeted protein structure modelling

A comprehensive 3D model of the targeted protein was predicted using trRosetta. This server utilized different template models for 3D modelling of SAP. The one which is selected for this study was modelled by incorporating the 2PSG_A protein from PDB. This tool provided crucial information about the protein's structural attributes. The model's confidence was notably high i.e., 100%, which increased its reliability in terms of accuracy. This high degree of confidence guided the selection of the first predicted structure, which was then downloaded to undergo further evaluation. In addition to this, the coverage score of 85.6% suggested the high homology between the query and the template sequence. This high fraction of coverage indicated that most of the sequence had a structural reference as well. Moreover, the The E-value of 4.1E-55 also revealed an extremely low probability of the fact that the observed alignment has occurred by random chance signifying the reliability of the predicted model of SAP protein. The Z-score of 16.365 also supported the outcome scores of the previously discussed factors which suggested the high significance of the modelled protein. This initial model provided a strong framework for further investigation of the functional attributes of the protein and its potential as a target for drug discovery initiatives. The Fig. 2 illustrates the predicted structure of the protein under study which is comprised of an efficient blend of crucial structural components including alpha helices and beta sheets.

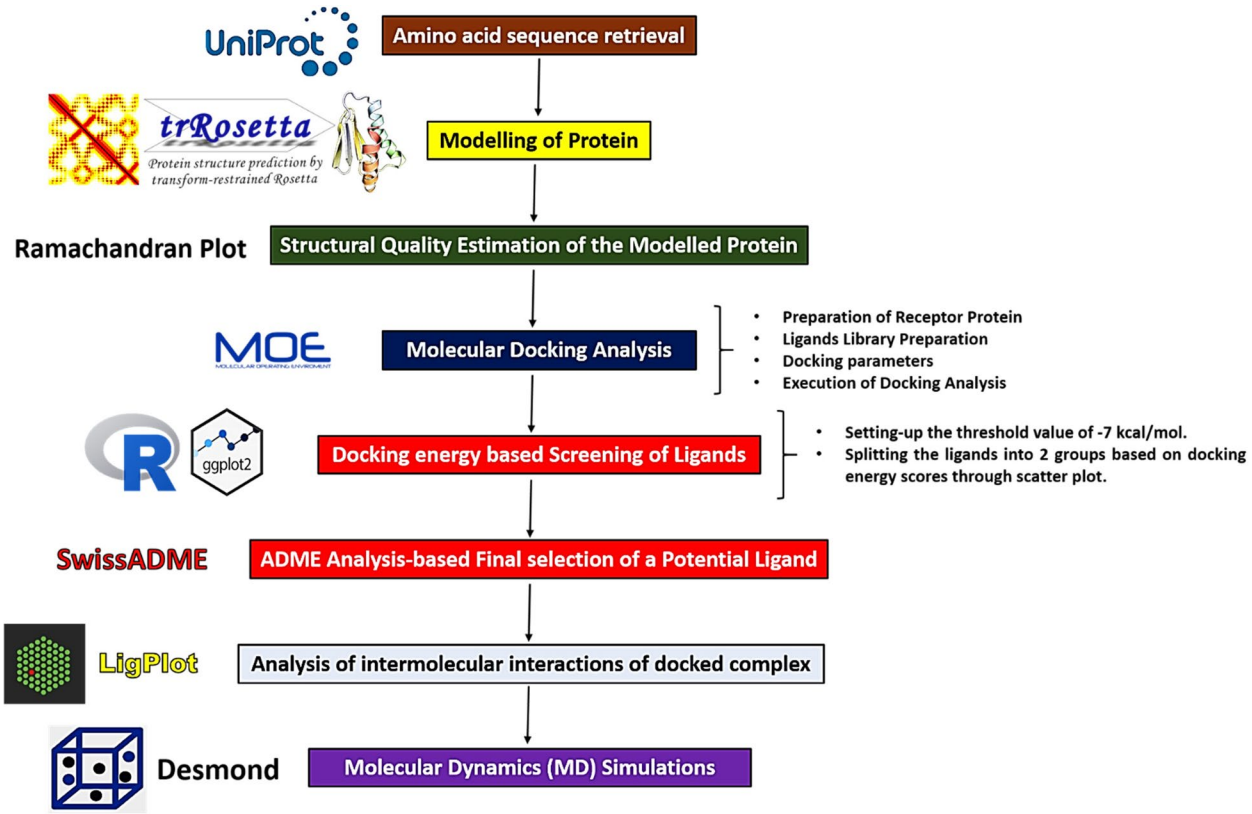

Fig. 1 The complete methodological workflow followed in this study

Fig. 2 The predicted 3D model of Secreted Aspartyl Proteinase (SAP) of *C. lusitaniae*

Protein structural validation

The Ramachandran plot is an important tool in structural biology to assess the conformational angles of amino acids in protein structures. The most favored combinations of the phi (f) and psi (?) angles were indicated by the red regions on the plot in the Fig. 3. These were the conformations that were sterically allowed and typically correlated to the alpha-helix and beta-sheet secondary structures in SAP's predicted structure. The presence of multiple residues in these regions predicted that the protein structure was stable and its quality was also appreciable. Adjacent to the red regions, there were yellow areas in the plot, which represented additionally allowed regions. This area corresponded to turns or loops in the protein structure. The white areas represented combinations of f and ? angles that were generally not allowed due to steric hindrance. Specified residues were annotated on the plot, such as "ALA + 3 1(A)" and "PASP + 5 1(A)". While, the results of the given structure of SAP suggested that the majority of the amino acid residues lied in the most favorable regions i.e., 92.7%, whereas, in the additionally allowed region the residues percentage was 6.2% and in the disallowed regions, there were only 0.9% residues which were allocated in this particular zone. Therefore, on the basis of the conclusive results, especially, the number of residues in the most favored regions thus gave an indication of the most stable conformation of the predicted structure of SAP, suggesting its better quality.

Screening and selection of a potential compound through molecular docking and pharmacokinetics analysis

The molecular docking analysis was used to identify potential compounds from the selected compounds that could effectively bind with SAP. Initially, the 3D structure

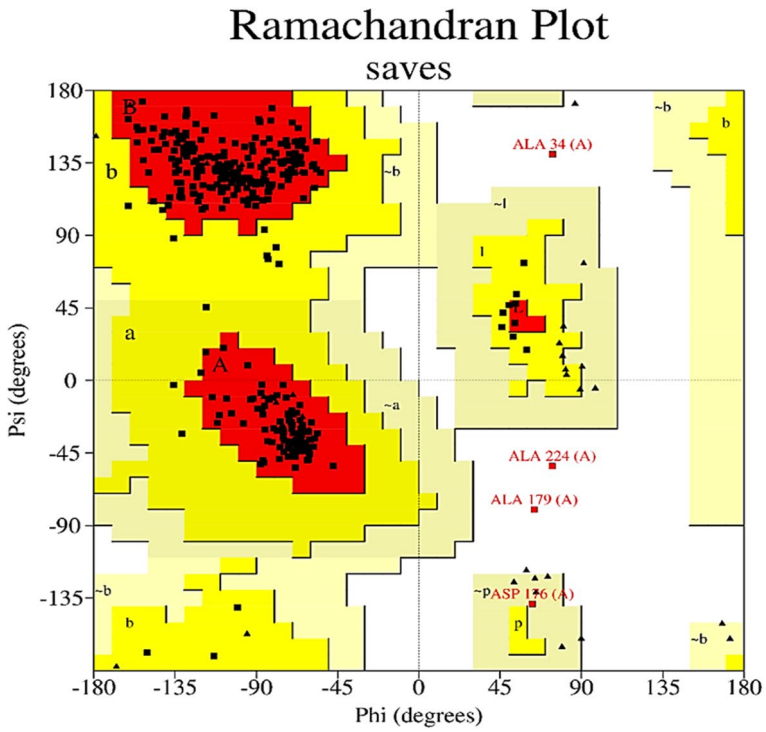

Plot statistics

Residues in most favoured regions [A,B,L]	319	92.7%
Residues in additional allowed regions [a,b,l,p]	21	6.1%
Residues in generously allowed regions [~a,~b,~l,~p]	1	0.3%
Residues in disallowed regions	3	0.9%
Number of non-glycine and non-proline residues	344	100.0%
Number of end-residues (excl. Gly and Pro)	2	
Number of glycine residues (shown as triangles)	35	
Number of proline residues	15	
Total number of residues	396	

Based on an analysis of 118 structures of resolution of at least 2.0 Angstroms and R-factor no greater than 20%, a good quality model would be expected to have over 90% in the most favoured regions.

Fig. 3 Ramachandran plot to assess the structural quality of the predicted 3D model of SAP. The scores of most favored region i.e., 92.7% indicated that the structure is stereochemically stable

of the protein was prepared and incorporated into the analysis to enable precise interactions with different phytochemicals. To evaluate the binding affinities of each ligand-protein complex, docking scores were computed. Lower scores indicated stronger binding affinities. The range of docking energy scores of all the docked complexes varied from -4.7561 kcal/mol. to -7.6327 kcal/mol. These varied docking scores, indicated different levels of interactions with the SAP. While, significant interactions were identified, including van der Waals forces, hydrophobic interactions, and hydrogen bonding. Deep penetration of certain ligands into the binding pocket resulted in multiple favorable interactions with important residues of amino acids. Comparative analysis of the interactions were made based upon their docking energies because the least energy scores proposed the better docking interactions and vice versa. This perspective highlighted another important fact that the docked complexes with the less docking energy values would be more stable than the rest ones. The Table 2 illustrates the binding energies (kcal/mol.) of each of the interacted compounds including the three approved anti-fungal drugs (Fosmanogepix, Opelconazole and Olorofim) which were included as control during the docking analysis. While,

Table 2 The scores of docking/binding energies of all of the incorporated compounds with SAP

Compounds	Docking Energy (kcal/mol.)
(-) -Epicatechin	-4.7561
Baicalin	-6.7106
Chloroquine	-6.2030
Chrysin 5,7-demethyl ether	-5.7949
curcumin	-6.0600
(-) _epigallocatechin 3-gallate	-6.5496
Galangin	-5.0213
Isorhamnetin	-5.4598
Malvidin	-5.6145
Nobiletin	-6.3605
Sinensetin	-6.7934
Tangeretin	-6.2037
5.7-dihyroxy 4-metroxyflavone	-5.3275
(+) -catechin	-5.5417
Luteolin	-4.9330
Quercetin	-5.4890
Epigenin	-5.5426
Pelargonidin	-5.1197
Genistein	-5.3526
Delphinidin	-5.2595
Hesperidin	-7.2614
Naringin	-8.1556
Daidzein 7-o-beta-D-glucoside	-6.3022
Fisetin	-5.6601
Nargingenin	-5.1344
Deoxycyclinemyricetin(1-)	-6.3156
Myricetin(1-)	-5.5372
Kaemferol oxoanion	-5.0305
Neohesperidin	-6.7393
(-)-epicatechin -3_0_gallate	-5.9686
(-) -gallocatechin	-4.7924
Cyanidin(1-)	-5.0445
Peonidin	-5.3770
Petunidin	-6.1504
Daidzin 4'-0-glucuronide	-7.6327
2-Coumaroylquinic acid	-6.6730
Apigenin	-5.9920
Biochanin A	-6.3745
Pinosylvin	-5.4615
Emodin	-5.7007
Pleosporone	-6.2230
Formononetin	-6.1939
Galangin	-5.8159
Glycitein	-6.4714
Homoeriodictyol	-6.3776
Licochalcone B	-6.4424
Licochalcone F	-7.0569
Morin	-6.2867
Oroxylin A	-6.1579
Pinocembrin	-5.8352
Rosmarinic acid	-5.8103
Scutellarein	-6.5068
Control Drugs (approved anti-fungal drugs)	
Fosmanogepix	-6.4315
Opelconazole	-7.6412
Olorofim	-6.9735

for better graphical representation of these results, R programming based scatter plot was also constructed which segregated the interacted ligands into two categories by creating a threshold value of -7.3 kcal/mol. This plot can be visualized in the Fig. 4. Since, this particular threshold value can ensure a significant level of interactions and binding affinities, therefore, only the docked complexes which exhibited the docking score equal to or lesser than -7.3 kcal/mol. were retained for the next phase of screening while, the rest of complexes were discarded. The compounds which were screened-out during this phase included opelconazole, daidzin 4'-0-glucuronide and naringin. Their respective docking scores can also be visualized in the Fig. 4.

The second screening phase which was in fact the final phase of selecting a potent compound was through the pharmacokinetics or ADME analysis. Thus, the selected compounds which included opelconazole, daidzin 4'-0-glucuronide and naringin were subjected to ADME investigation by employing the SwissADME server (http://www.swissadme.ch/). This crucial stage incorporated several parameters to evaluate these three compounds including the water solubility, pharmacokinetic properties, CYP450 inhibitor status and most importantly, the Lipinski rule. All of the results of four compounds under considerations suggested that only the daidzin 4'-0-glucuronide followed all of the required pharmacokinetic and drug-likeness attributes. Moreover, it was also noteworthy that daidzin 4'-0-glucuronide not only fulfilled the required drug-likeness properties but also, it exhibited significantly considerable docking score i.e., -7.6327 kcal/mol. which suggested that this compound could be a promising natural compound which could inhibit the pathogenic characteristic of secreted aspartyl proteinase (SAP) of *C. lusitaniae*. It is important to mention here that daidzin 4'-0-glucuronide has not been employed as an anti-fungal drug yet signifying the

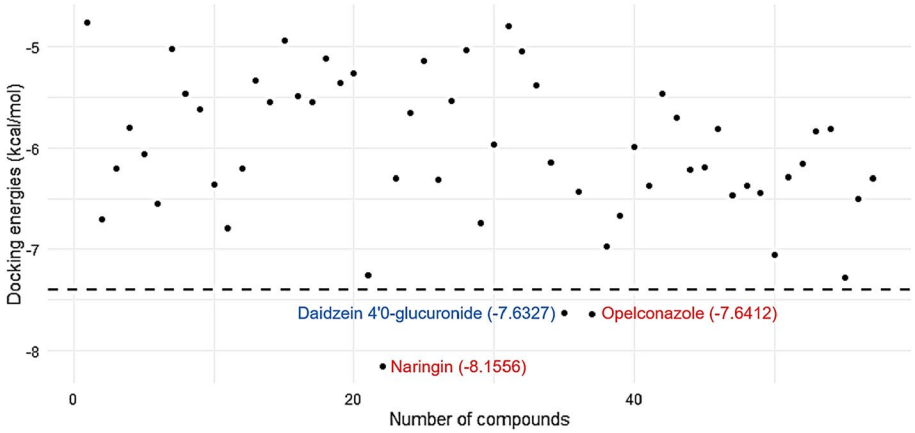

Fig. 4 Scatter plot to segregate and screen-out the ligands/compounds on the basis of docking energy scores. A threshold value of -7.3 kcal/mol. was set to segregate the best-docked compounds

novelty of work, however, its efficacy has been explored in various other therapeutic settings. Although, only computational techniques have been applied to study this particular domain of daidzin 4'-0-glucuronide which might be of a limited significance but still the findings of this study provides with the direction towards *in-vivo* and *in-vitro* validations. While, the results of ADME analysis oriented final scrutiny can be visualized in the Table 3.

Afterwards, different docking representations of the finalized docked complex i.e., SAP-daidzin 4'-0-glucuronide were computed to infer the specified amino residues of SAP which were involved in this interaction. The Fig. 5 (a) demonstrates the three dimensional (3D) docking representation of SAP-daidzin 4'-0-glucuronide docked complex whereas, the Fig. 5 (b) represents the 2D docking interactions. It can be observed from both of the figures that GLY139, ASP357, THR358, ARG62, ASP278, ASP140, TYR138 and ILE181 were the specified amino acids which were involved in the docking interaction. The latter one also exhibits the respective distances between the interacting receptor atoms and the ligand.

Lig-plot analysis of SAP-daidzin 4'-0-glucuronide complex

Ligplot was used to analyze the intermolecular interactions, including hydrogen bonding and hydrophobic interactions in the docked complex of SAP and daidzin 4'-0-glucuronide. Among the most potent kinds of non-covalent interactions were the hydrogen bonds. In the context of the lig-plot, hydrogen bonds are formed when a hydrogen atom, covalently bonded to a highly electronegative atom like nitrogen or oxygen, is also attracted to another electronegative atom from the ligand or protein. In the Fig. 6, the black balls represented carbon atoms form the backbone of the ligand structure, while the red balls (oxygen) and blue balls (nitrogen) indicated functional groups that participate in hydrogen bonding and other interactions. The amino acids Asp101, Asp140, Thr281, Arg262, Thr358, Asp356, and Asp357 were involved in forming these bonds with the ligand (daidzin 4'-0-glucuronide), which suggested that they were the key residues for the ligand's binding. The SAP formed six hydrogen bonds (H bonds) with the daidzin 4'-0-glucuronide while, the O_2 atoms of the ligand was engaged in a H-bond with the side chain of Arg62, Thr338, Asp357 and Asp356 amino acid of SAP. The formation of these H-bonds was further characterized by the average distances between the corresponding heavy atoms and also, by the percentage of occurrence during simulations. Moreover, in addition to the hydrogen bonding interactions, the ligand was involved in the hydrophobic interactions too. Hydrophobic Interactions occurred between nonpolar molecules or parts of molecules, which tend

Table 3 The results of analysis major drug-likeness attributes of the screened-out compounds for final selection

Sr. no	Names of the Selected Compounds	Pharmacokinetic properties (fulfilled/not fulfilled)	Water solubility (Yes/No)	CYP450 inhibitor (Yes/No)	Lipinski rule (followed/violated)
1	***Opelconazole***	Not fulfilled	No	Yes	Violated
2	***Daidzin 4'-0-glucuronide***	Fulfilled	Yes	No	Followed
3	***Naringin***	Not fulfilled	Yes	No	Violated

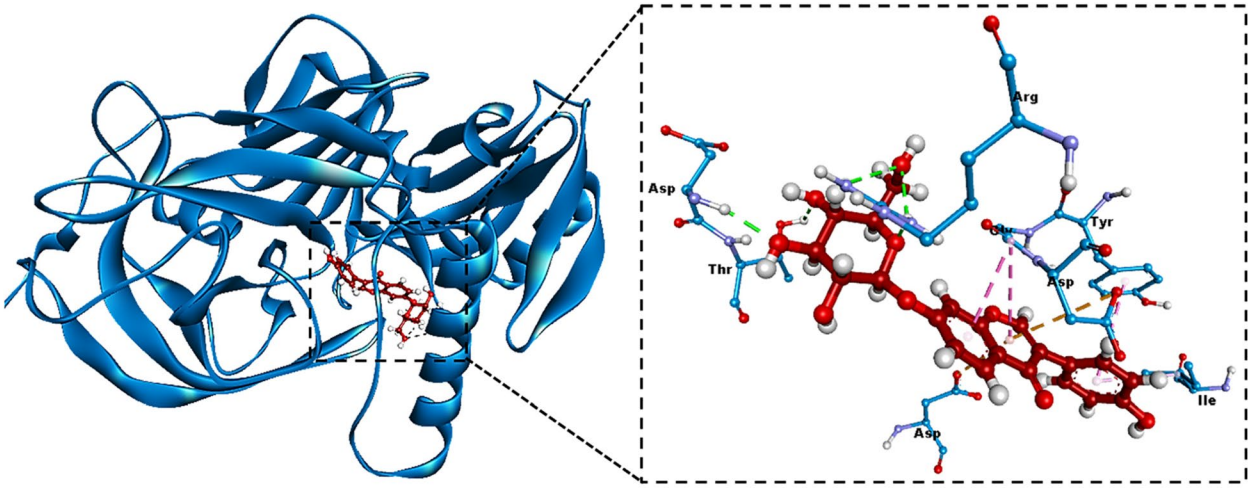

(a)

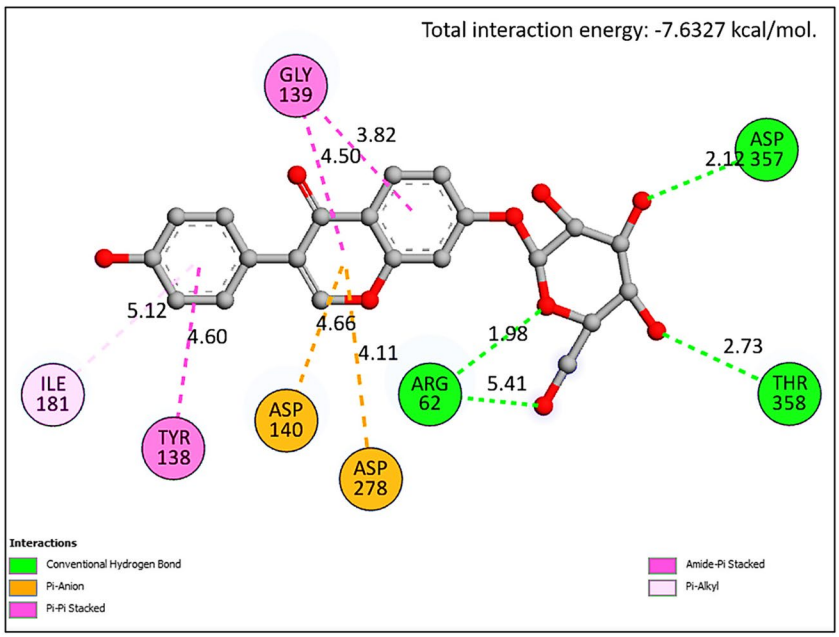

(b)

Fig. 5 **a** Three dimensional (3D) docking representation of SAP-daidzin 4'-0-glucuronide complex. **b** Two dimensional (2D) illustration of SAP-daidzin 4'-0-glucuronide, showing various types of interactions occurred, along the respective distances between the ligand and the corresponding interacting receptor atoms

to avoid contact with water (hydrophobic effect). In the lig-plot, the eyelash-like lines pointing towards the ligand from Thr 281, Asp140, Asp101, Val99, Ilel81, Ile78, Gly280, Ile360 and Gly139 indicated areas where hydrophobic interactions helped to stabilize the ligand within the binding pocket. These interactions were less about direct contact and more about creating an environment where water was excluded, thus favoring the ligand binding. The specific amino acids involved in interactions with the ligand suggested that the protein had a particular binding site that was complementary to the shape and chemical properties of daidzin 4'-0-glucuronide. This specificity was crucial for the biological function of the protein, as it ensures that it interacts with the correct ligand. The hydrogen bonds and hydrophobic interactions depicted in the lig-plot contributed to the stability of the protein–ligand complex. A stable complex is often necessary for the proper biological activity of the protein, such as enzyme catalysis or signal transduction. For researchers in drug design, understanding these

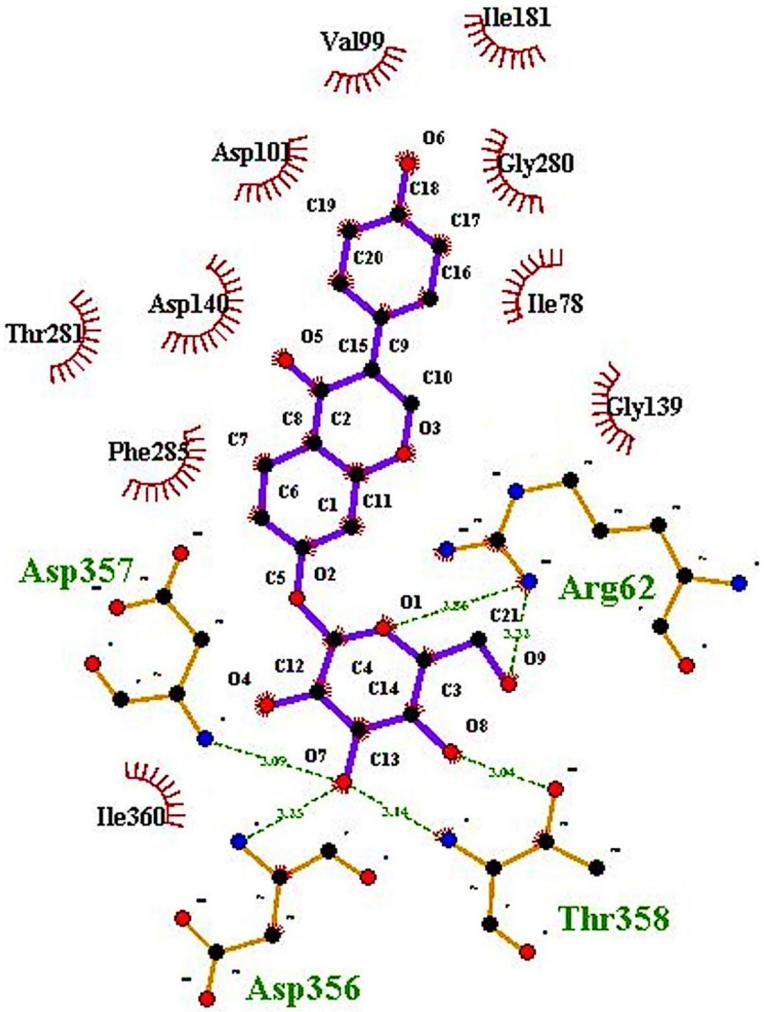

Fig. 6 LigPlot results to get deep insights regarding the interactions occurred during molecular docking between SAP and daidzin 4'-0-glucuronide

interactions provides the insights into how modifications to the ligand could improve its binding affinity or selectivity for the given protein.

Elaborative pharmacokinetic analysis of the selected compound 'daidzin 4'-0-glucuronide' and its comparative analysis with approved anti-fungal drugs

After the docking analysis, three of the phytochemicals were shortlisted and their corresponding ADME characteristics were assessed using SwissADME. Daidzin 4'-0-glucuronide showed the best pharmacokinetic and physicochemical properties than the rest of the selected compounds. Given its potential, further exploration of the ADME properties was deemed crucial to unveil its medicinal or drug-like attributes. Some of the key features of this compound are illustrated in Fig. 7, especially with regard to bioavailability radar which showed that the given compound possessed the insaturation and polarity characteristics. This fact indicated that daidzin 4'-0-glucuronide would not only be more reactive but also, it will be more water soluble and would also be excreted out of the body. These properties initially signified that the compound under study had significant drug-like potential.

Afterwards, the physicochemical properties of daidzin 4'-0-glucuronide were revealed, exhibiting several distinct characteristics which included that the molecule was large, including 30 heavy atoms, 16 of which were aromatic, and had a molecular weight of 416.38 g/mol. suggesting that this compound was structurally complex. This fact was assured by the score of sp3-hubridized carbons which was 0.29, suggesting it to be a moderately complex molecular structure.

Moreover, daidzin 4'-0-glucuronide possessed nine hydrogen bond acceptors, five hydrogen bond donors, and five rotatable bonds which indicated that significant flexibility and the possibility of intermolecular

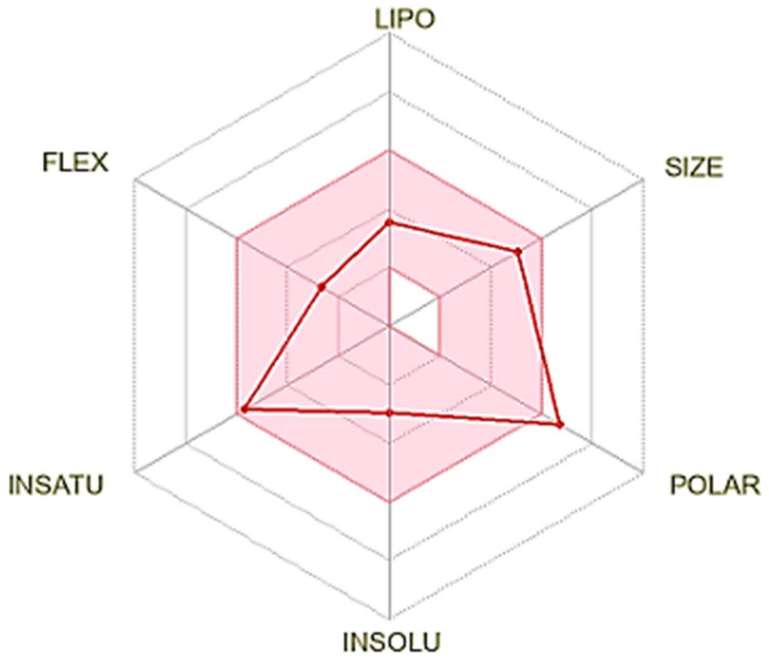

Fig. 7 Bioavailability radar of daidzin 4'-0-glucuronide, showing a degree of insaturation (INSATU) and polarity (POLAR)

interactions were present in its molecular structure. Regarding the lipophilicity, an average affinity for lipid environments was indicated by the consensus log *P* value of 0.63. ESOL log S value of -2.97 and Silicos-IT log S value of -3.28 showed that this property was supported by more effective water solubility. It was predicted that daidzin 4'-0-glucuronide would have moderately less gastrointestinal (GI) absorption and would not cross the blood–brain barrier (BBB) as well.

Furthermore, daidzin 4'-0-glucuronide was shown to be a substrate for P-glycoprotein (Pgp). Analysis of excretion and metabolism provided more informative insights in which it was not predicted that daidzin 4'-0-glucuronide would inhibit any of the key cytochrome P450 enzymes (CYP1A2, CYP2C19, CYP2C9, CYP2D6, CYP3A4), suggesting a decreased risk of drug-drug interactions, mediated by these enzymes. On the other hand, its calculated skin permeability coefficient (log Kp) was -8.36 cm/s, signifying its low skin permeability. In the end, some of the additional relevant features were also examined in this context. It was determined that daidzin 4'-0-glucuronide did not violated the Lipinski's rule-of-five, zero of Ghose's, one of Veber's, one of Egan's, and three of Muegge's. With a bioavailability score of 0.55, modest oral bioavailability was indicated. Notably, the molecule did not show either Brenk or PAINS signals while, its synthetic accessibility score was 5.01, suggesting a very moderate level of synthetic complexity. All of the above explained parameters along their respective results are demonstrated collectively in the Table 4.

Moreover, to further authenticate and highlight the significance of the findings of this work, the comparative pharmacokinetics analysis of daidzin 4'-0-glucuronide and some of the market approved traditional anti-fungal drugs is also performed in this study. The Table 4 displays the elaborative drug properties of three approved antifungal drugs (fosmanogepix, opelconazole and olorofim) and daidzin 4'-0-glucuronide. It can be observed that none of the approved drugs completely follow all of the required crucial pharmacokinetics properties. The fosmanogepix exhibited poor water solubility and inhibition against two of the CYP450 isoforms. Similarly, the opelconazole was found to be insoluble in water and showed inhibition against three CYP450 isoforms. Most importantly, it violated the Lipinski rule, which is highly pivotal while estimating the drug perspective of a compound. Furthermore, the olorofim found to be moderately soluble in water and exhibited inhibition against four CYP450 isoforms. While, daidzin 4'-0-glucuronide almost completely followed not only the previously discussed parameters but also other crucial factors which indicates the importance and significance of the findings of this work and daidzin 4'-0-glucuronide, to be a probable anti-fungal phytocompound. The results of this comparative analysis are demonstrated in the Table 5.

Table 4 An elaborative analysis of pharmacokinetics and other drug-likeness characteristics of Daidzin 4'-0-glucuronide including, physicochemical properties, lipophilicity and solubility status, analysis of pharmacokinetics, drug likeness and medicinal chemistry properties

Physiochemical Properties	
Molecular weight	416.38 g/mol
No. of heavy atoms	30
No. of aromatic heavy atoms	16
Fraction Csp3	0.29
No. of rotatable bonds	4
No. of H-bond acceptors	9
No. of H-bond donors	5
Molar Refractivity	104.09
Topological polar surface area (TPSA)	149.82 A2
Lipophilicity	
Consensus Log P	0.63
Log $P_{o/w}$ (iLOGP)	2.42
Log $P_{o/w}$ (XLOGP3)	0.67
Log $P_{o/w}$ (WLOGP)	0.34
Log $P_{o/w}$ (MLOGP)	-1.11
Log $P_{o/w}$ (SILICOS-IT)	0.82
Solubility	
Log (ESOL)	-2.97
Solubility	4.42e-01 mg/ml; 1.06e-03 mol/l
Class	soluble
Log s (Ali)	-3.39
Solubility	1.69e-01 mg/ml; 4.05e-04 mol/l
Class	soluble
Log S(SILICOS-IT)	-3.28
Solubility	2.18e-01 mg/ml; 5.22e-04 mol/l
Class	soluble
Pharmacokinetics	
GI absorption	Moderately low
BBB permeant	No
P-gp substrate	No
CYP1A2 inhibitor	No
CYP2C19 inhibitor	No
CYP2C9 inhibitor	No
CYP2D6 inhibitor	No
CYP3A4 inhibitor	No
Log Kp (skin permeation)	-8.36 cm/s
Drug likeness	
Lipinski	Yes; 0 violation
Ghose	Yes
Muegge	Yes; no violation
Bioavailability Score	0.55
Medicinal Chemistry	
PAINS	0 alert
Brenk	0 alert
Leadlikeness	No
Synthetic accessibility	5.01

Molecular dynamics simulations

Root mean square deviation (RMSD)

Comparative RMSD analysis by including the top hits from the phytocompounds library and the reference/marketed approved drugs In the RMSD analysis of the three complexes over a 200 ns simulation, each ligand daidzin 4'-0-glucuronide, hesperidin, and naringin displayed distinct interaction stability with the SAP protein. The daidzin 4'-0-glucuronide-SAP complex Fig. 8 (a) exhibited an initial phase of low fluctuations, suggesting a stable binding configuration early on. While minor increases in RMSD occurred mid-simulation, these fluctuations indicate slight conformational adjustments, likely as the ligand adapted within the SAP binding site. Importantly, daidzin 4'-0-glucuronide achieved a more equilibrated and stable interactions until the end of simulations, affirming its suitability as a well-fitted compound for SAP binding. In contrast, the hesperidin-SAP complex Fig. 8 (b) showed higher initial RMSD values, possibly reflecting a less stable initial binding mode. Hesperidin might not achieve the same binding stability as daidzin 4'-0-glucuronide, as seen by significant fluctuations in the mid-simulation phase which suggested larger conformational changes and only partial stabilization by the end of the simulations. Throughout the simulation, the naringin-SAP complex Fig. 8 (c) showed decreased, suggesting a stable binding profile than the hesperidin. The daidzin 4'-0-glucuronide-SAP complex, on the other hand, not only maintained stable interactions but also showed favorable adaptability within the SAP binding pocket, highlighting it as the best-screened compound among the three ligands due to its strong binding affinity and stability with SAP.

Afterwards, another MD simulation analysis was performed to compare the daidzin 4'0-glucuronide with the approved anti-fungal drugs. These drugs included the fosmanogepix, olorofim and opelconazole. The comparative MD simulation results of all the four complexes displayed varied behavior throughout the 200 ns time frame. Initially, in context of SAP-daidzin 4'-0-glucuronide, the RMSD of SAP started at approximately 1.8 Å and showed a gradual increase, stabilizing around 3.6–4.0 Å after 75 ns. This suggested that the protein underwent initial conformational changes but achieved relative structural stability after this point in the simulation. The fluctuations observed between 100–150 ns likely represented localized adjustments in the protein structure but did not indicate significant instability overall. On the other hand, the ligand daidzin 4'-O-glucuronide exhibited relatively stable RMSD values between 2.0 and 3.5 Å throughout the simulation, with fewer fluctuations compared to the

Table 5 The comparative analysis of drug properties of fosmanogepix, opelconazole, olorofim and daidzin 4′-0-glucuronide. The overall results affirmed that the compound under study in this work (daidzin 4′-0-glucuronide) followed all of the required parameters

Parameters	Fosmanogepix (Approved in 2022)	Opelconazole (Approved in 2023)	Olorofim (approved in 2023)	Daidzin 4′-0-glucuronide
Solubility				
Log S (ESOL)	-3.72 Soluble	-7.81 Poorly soluble	-5.56, moderate soluble	-2.97 soluble
Log S(Ali)	-4.00 1.17e-02 mg/ml Moderately soluble	-7.90 Poorly soluble	-5.63 moderate soluble	-3.39 soluble
Log S (SILICOS-IT)	-6.28 Poorly soluble	-11.85 Insoluble	- 8.20, poorly soluble	-3.28 soluble
Pharmacokinetics				
BBB permeant	No	No	No	No
P-gp substrate	Yes	No	Yes	No
CYP1A2 inhibitor	No	No	No	No
CYP2C19 inhibitor	Yes	No	Yes	No
CYP2C9 inhibitor	No	Yes	Yes	No
CYP2D6 inhibitor	No	Yes	Yes	No
CYP3A4 inhibitor	Yes	Yes	Yes	No
Druglikeness				
Lipinski's Rule	Yes; 0 violation	No; 2 violations (MW > 500, LogP > 4.15)	Yes; 0 violation	Yes; 0 violation
Ghose Filter	Yes	No; 4 violations: MW > 480. WLOPG > 5.6, MR > 130	No 2 violations (MW > 480, MR > 130)	Yes
Muegge Rules	No; 1 violation (TPSA > 150)	No, 2 violation: MW > 600, XLOGP3 > 5	Yes	Yes
Bioavailability Score	0.11	0.17	0.55	0.55
Medicinal Chemistry				
Synthetic Accessibility	4.45	5.27	3.65	5.01

protein as shown in the Fig. 9 (a). This indicated that the ligand maintained a stable binding conformation within the binding pocket of the SAP protein for the majority of the simulation time. Whereas, in case of SAP-fosmanogepix complex, the RMSD of the protein showed a gradual rise during the first 50 ns of the simulation, stabilizing at around 4.5 Å. This indicated that the protein structure underwent some conformational changes initially but eventually reached equilibrium, with minimal fluctuations beyond the 100 ns mark. The consistent RMSD values after stabilization suggested that the SAP protein maintained its overall structural integrity throughout the simulation. However, the RMSD of the fosmanogepix ligand fluctuated significantly more, compared to the protein. Initially, the ligand RMSD aligned with the protein's fluctuations, suggesting strong interactions. But, after around 100 ns, a notable drop in ligand RMSD was observed, reaching values below 4 Å which can be observed in Fig. 9 (b). This drop indicated that the ligand either repositioned itself or found a more stable binding mode within the binding pocket of the SAP protein. The reduced RMSD values in the later stages suggested that the ligand was more firmly accommodated within the binding site, possibly achieving a stable binding conformation. On the contrary, SAP-olorifim presented a bit different kind of simulation results. At the start of the simulation, both the SAP protein and the ligand exhibited low RMSD values, indicating that their initial configurations were well-conserved. The protein RMSD increased rapidly within the first 20 ns, reaching around 2.5 Å. This increase was indicative of the protein adapting to the solvent environment and undergoing initial conformational changes. After this adjustment phase, the RMSD stabilizes around 2.5–3.0 Å with slight fluctuations, which suggested that the protein structure remained stable with minimal deviations throughout the simulation. While, the ligand RMSD remained relatively low and stable, fluctuating between 1.0 Å and 2.5 Å. This indicated that olorofim remained securely bound in the protein's active site, maintaining a stable conformation with no significant drift away from its binding pocket. Whereas, in case of SAP- opelconazole complex, the protein maintained a fairly stable RMSD throughout the 200 ns trajectory. Initially, the protein RMSD started near 1.5 Å

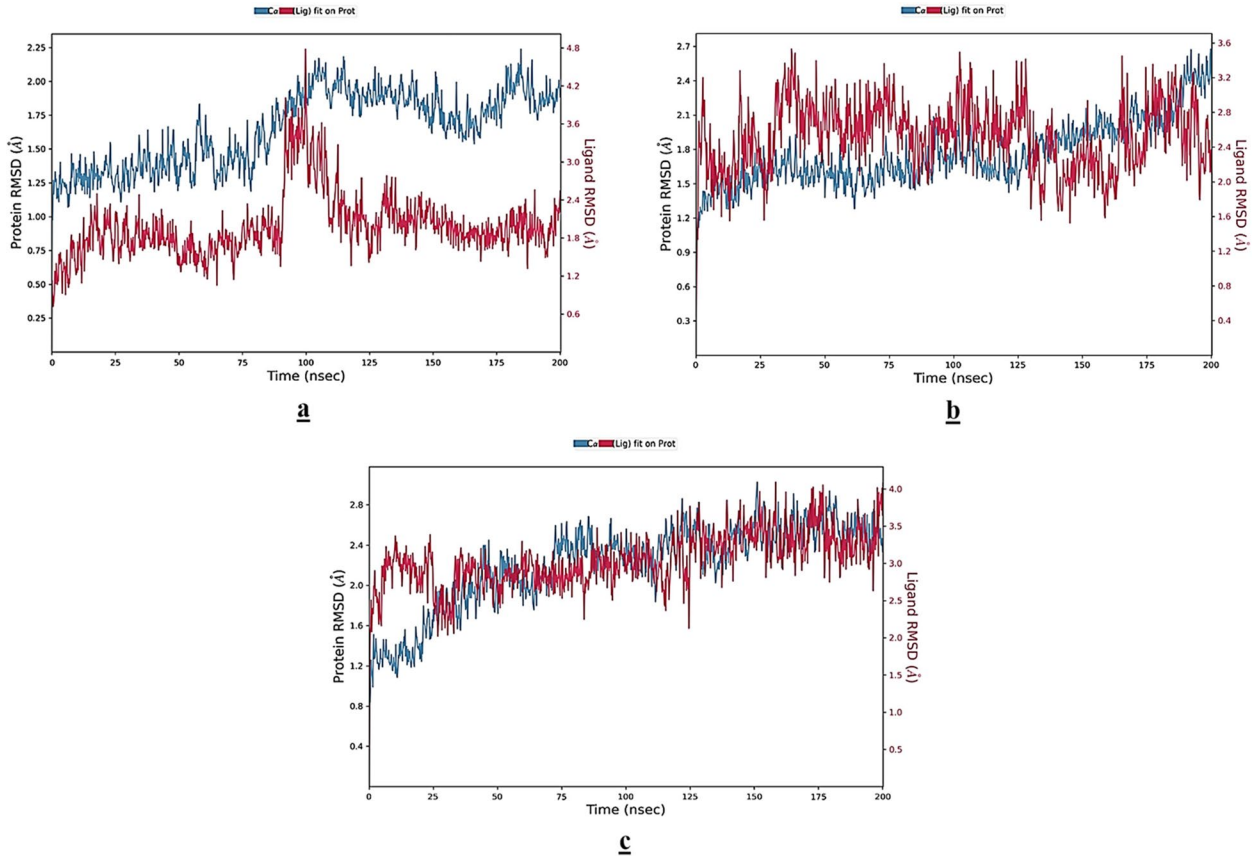

Fig. 8 The representation of root mean square deviation graphs (**a**): SAP-daidzin 4′-O-glucuronide complex; (**b**): SAP-hesperidin complex; (**c**): SAP-naringin complex

and fluctuated between 2.4 Å and 4.8 Å. The rise around 100–175 ns suggested some conformational adjustments. However, the average deviation remained under control, indicating that the protein did not undergo any dramatic conformational changes and remained structurally stable during the simulation. While, the ligand RMSD started at around 1 Å and displayed a gradual rise, fluctuating between 2 Å and 7 Å after the first 50 ns. These fluctuations indicated that the ligand underwent some movement within the binding pocket. Despite this, it did not show signs of complete dissociation, as it stabilized after 150 ns, maintaining an RMSD below 6 Å. The movements observed likely reflect adjustments to optimize binding interactions. These overall results are compiled in the Fig. 9 which suggested that the SAP- daidzin 4'-O-glucuronide complex exhibited superior stability and performance compared to the other three complexes analyzed. Its consistent protein and ligand RMSD values, along with minimal residue fluctuations in key binding regions, underscored its potential as a highly stable interaction. These results suggested that daidzin 4'-O-glucuronide could be a promising candidate for further drug discovery and development targeting SAP.

Root mean square fluctuation (RMSF)

Comparative RMSF analysis by including the top hits from the phytocompounds library and the reference/marketed approved drugs In the RMSF (Root Mean Square Fluctuation) analysis of SAP with three different ligands, daidzin 4'-0-glucuronide, hesperidin, and naringin, the RMSF plots provided insight into the flexibility and stability of each complex. For daidzin 4'-0-glucuronide (Fig. 10a), the RMSF values demonstrated relatively stable fluctuations with minor peaks, indicating strong binding stability in the SAP active site and limited residue mobility throughout the protein. This implied a consistent interaction between daidzin 4'-0-glucuronide and SAP, suggesting enhanced stability in the complex. Hesperidin (Fig. 10b) showed a few larger fluctuations, particularly in some loop regions, which might suggest slightly less stable interactions compared to daidzin 4'-0-glucuronide. However, the overall RMSF values for hesperidin

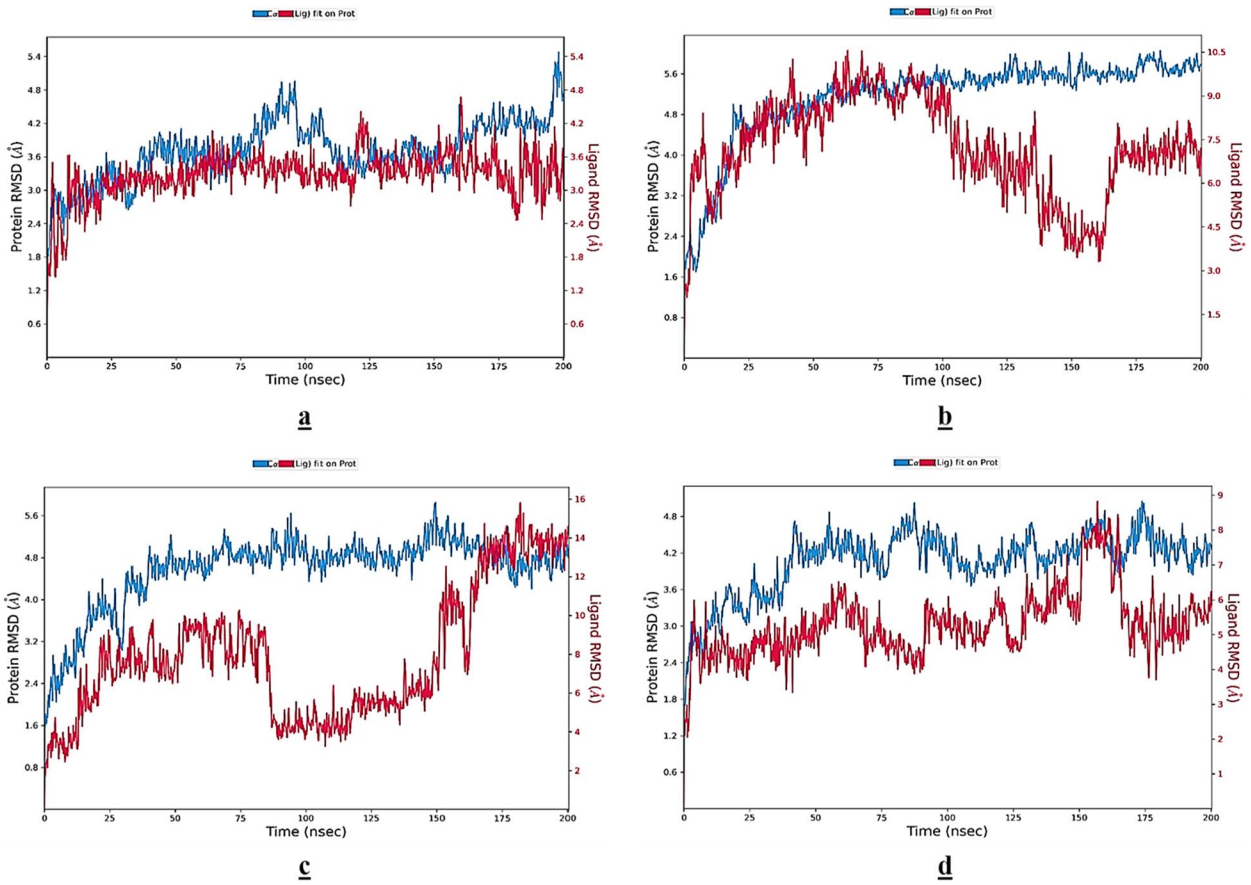

Fig. 9 Illustration of root mean square deviation graphs (**a**): SAP-daidzin 4'-O-glucuronide complex; (**b**): SAP-fosmanogepix complex; (**c**): SAP-olorofim complex; (**d**): SAP-opelconazole complex

remained within a reasonable range, implying moderate stability. For naringin (Fig. 10c), there was notable fluctuation at specific residues, reflecting less stability in comparison to daidzin 4'-0-glucuronide and indicating weaker interactions at certain SAP binding sites. In conclusion, daidzin 4'-0-glucuronide demonstrated the most favorable RMSF profile among the three ligands, exhibiting minimal fluctuations and consistent stability in the SAP complex. This overall outcome suggested the daidzin 4'-0-glucuronide to be the most appropriate compound based on the RMSF analysis, aligning with its selection as the most promising screened compound.

While, in the second round of simulations, the RMSF plot (Fig. 11 (a)) shows that the SAP protein has significant fluctuations at the N-terminus, with values reaching as high as 6.4 Å while simulating with daidzin 4'-O-glucuronide. This suggested that the N-terminal region of the protein was highly flexible throughout the simulation. After residue 50, the fluctuations reduced significantly, remaining below 2.0 Å for the majority of the residues, indicating a stable and less flexible structure in these regions. Notable peaks around residues 100 and 300 showed increased flexibility, which could correspond to loop regions or areas of the protein that underwent conformational changes. These regions might be important for ligand (daidzin 4'-O-glucuronide) binding or the overall dynamics of the protein. Overall, the majority of the SAP protein appeared to be relatively stable, with only specific regions exhibiting higher flexibility. This suggested that the protein maintained its structural integrity during the simulation, except for the identified flexible regions. Where, in case of SAP-fosmanogepix complex, the residues at the N-terminal and in the range of approximately 50 to 100 showed the highest fluctuations, with values reaching up to 8 Å. These regions likely corresponded to loop regions or surface-exposed residues, which were inherently more flexible compared to the core of the protein. High flexibility in these regions might indicate potential sites for interaction with the ligand (fosmanogepix) or areas of conformational adaptability. The majority of the residues, especially those in

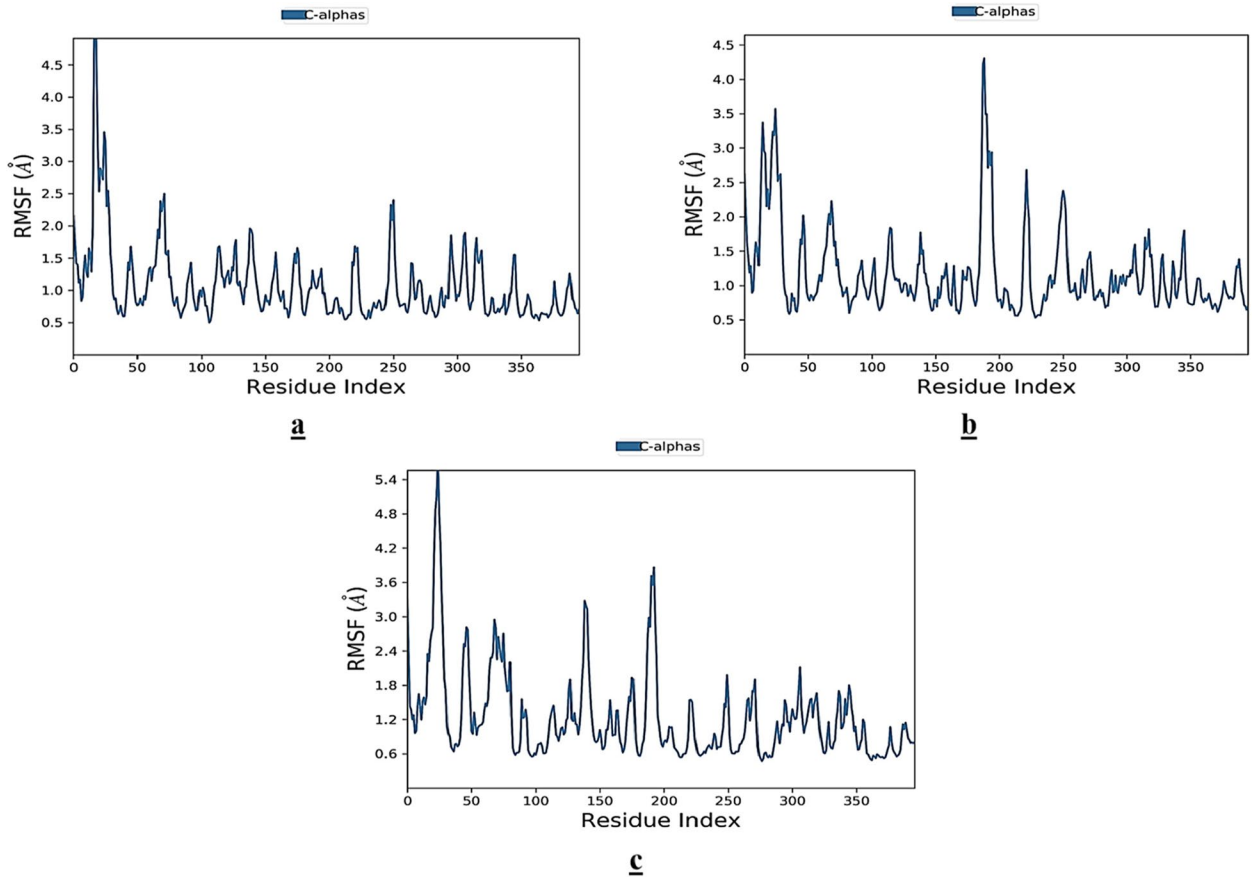

Fig. 10 The illustration of root mean square fluctuation graphs (**a**): SAP-daidzin 4'-O-glucuronide complex; (**b**): SAP-hesperidin complex; (**c**): SAP-naringin complex

the middle and C-terminal regions, exhibited relatively low RMSF values (around 1–2 Å). These stable regions are indicative of a well-folded core, where the structure remained rigid during the simulation. These fluctuations can be observed in the Fig. 11 (b). Furthermore, the RMSF map represented a bit different fluctuating fashion in the perspective of SAP-olorofim complex in which certain residues showed prominent peaks, particularly those located around residue indices 100, 180, and 300 (Fig. 11 (c)). These regions exhibited high RMSF values (above 3 Å), suggesting they were more flexible and might correspond to loop regions or surface-exposed areas of the protein. Such flexibility was typical in regions not directly involved in ligand binding or structural stability, allowing these segments to undergo larger conformational changes. However, between these peaks, several regions maintained relatively low RMSF values also, generally below 1.5 Å. These stable regions likely represented the areas involved in secondary structure elements, such as alpha-helices or beta-strands, or regions involved in the binding interactions with the ligand (olorofim). The reduced fluctuation in these areas indicateed that these residues were structurally constrained. Whereas, the SAP-opelconazole complex illustrated different results in this scenario. The majority of the protein residues in this regard exhibited low fluctuations (< 2 Å), indicating rigid and stable regions. Higher fluctuations were observed at the N-terminal and C-terminal regions, with a peak near the N-terminus exceeding 7 Å (Fig. 11 (d)), which could indicate unstructured or flexible regions.

After ensuring the significant structural stability and flexibility of daidzin 4'-O-glucuronide among both of the contexts, the detailed SSE and protein ligand interactions analysis was performed. In these particular analyses, daidzin 4'-O-glucuronide were underwent detailed investigation along the reference compounds (fosmanogepix, olorofim, opelconazole).

Secondary structure elements (SSE)

The graph in Fig. 12 shows a significant proportion of residues of the SAP protein while simulating with daidzin 4'-O-glucuronide adopting alpha-helical conformations, particularly around residue indices 50–100 and 200–350. The dominance of blue bars in these regions indicated a

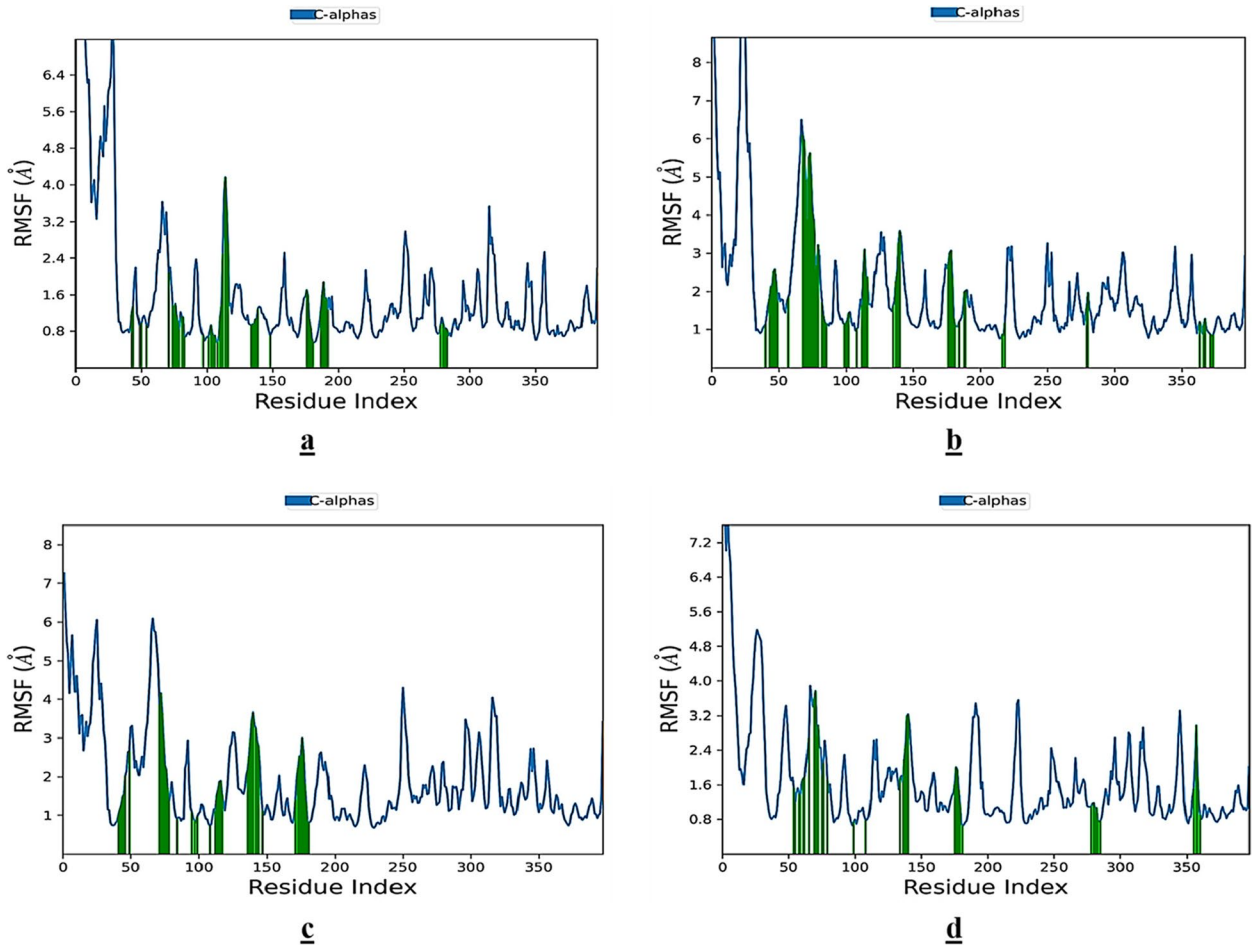

Fig. 11 The representation of root mean square fluctuation graphs (**a**): SAP-daidzin 4′-O-glucuronide complex; (**b**): SAP-fosmanogepix complex; (**c**): SAP-olorofim complex; (**d**): SAP-opelconazole complex

well-defined alpha-helical structure in these areas, with a high percentage of SSE. While, beta-strands were primarily located around residue indices 0–50, 150–200, and 300–350. These regions exhibited more orange bars, which indicated that these sections of the protein favored a beta-strand conformation. The alternation between blue and orange bars throughout the protein reflected a mixture of alpha-helices and beta-strands, indicative of a typical fold. The persistent height of the bars suggested that both the alpha-helices and beta-strands maintained their structure throughout the simulation, showing the structural stability of the protein's secondary elements. This fluctuated behavior of the SAP can be observed in the Fig. 12 (a). Whereas, in case of SAP- fosmanogepix complex, many regions showed persistent alpha-helical structures, particularly around residues 10–40, 150–180, and 300–350, where the blue bars remained consistently high, indicating stable helices. Moreover, the beta-strands were also prominently featured, particularly in regions such as 40–70 and 200–250, where red bars dominated. These regions reflected the stability of beta-strands, showing minimal transition to other structures. Additionally, there were some mixed or flexible regions where the blue and red bars fluctuated, indicating transitions between secondary structures. For instance, around residues 50–100 and 250–280, the graph showed variation, suggesting these areas underwent conformational changes which can be observed in the Fig. 12 (b). Furthermore, the SSE graph in context of SAP- olorifim complex revealed alternating patterns of alpha-helices and beta-strands throughout the SAP protein structure, with certain regions showing persistent secondary structures. These regions likely contributed to the protein's overall stability during the simulation. Notably, there were well-defined regions of both alpha-helices and beta-strands between residues 0–50, 150–200, and 300–350. This dynamic behavior can be visualized in the Fig. 12 (c). These consistent structures indicated that these sections of the protein were particularly stable and played a critical role in maintaining the overall conformation

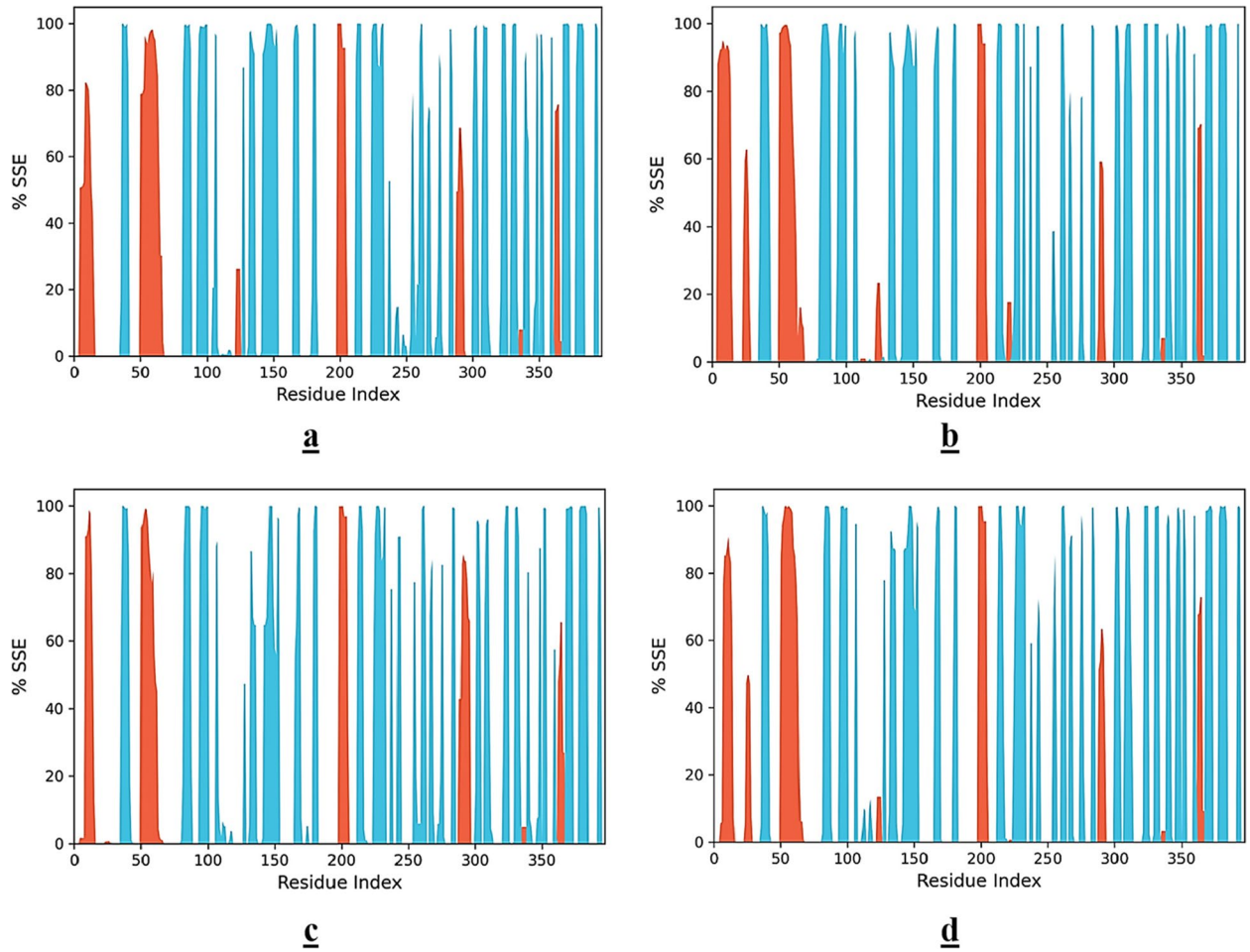

Fig. 12 Secondary structure elements (SSE) graphs (**a**): SAP-daidzin 4'-O-glucuronide complex; (**b**): SAP-fosmanogepix complex; (**c**): SAP-olorofim complex; (**d**): SAP-opelconazole complex

of SAP. In contrast, there were also some of the gaps between the SSE regions, which could correspond to loop regions or flexible areas that underwent more significant conformational fluctuations during the simulation. Afterwards, such dynamic transitions between SSE were also observed in context of SAP-opelconazole complex in which it can be seen that large portions of the SAP protein maintained well-defined alpha-helical structures, with multiple regions showing a high percentage of helicity (near 100% SSE) (Fig. 12 (d)). These continuous regions of alpha-helices indicated significant structural stability in these sections of the protein, essential for maintaining the conformation of SAP. Moreover, there were also several well-preserved beta-strands within the SAP structure, with some regions maintaining a high percentage of beta-strand content. This suggested a stable beta-sheet structure in these areas, further supporting the rigidity of certain regions of the protein.

Protein-ligand contacts

The graph (Fig. 13 (a)) illustrated the protein-ligand interactions between SAP and daidzin 4'-O-glucuronide over the course of a molecular dynamics simulation. Different types of interactions were depicted, majorly including the hydrogen bonds and hydrophobic interactions. Hydrogen bonds were highly prevalent in several residues, particularly around residues ASP77, SER105, ASP106, ASP135, and ALA179. These regions showed significant and consistent hydrogen bonding throughout the simulation, implying strong and stable interactions between SAP and daidzin 4'-O-glucuronide. While, residues such as TRP108, and ILE181, were notably involved in hydrophobic interactions, suggesting that these regions contributed to the overall binding stability by facilitating nonpolar interactions with the ligand (daidzin 4'-O-glucuronide). Furthermore, in case of SAP-fosmanogepix complex hydrogen bonds were seen frequently for residues like ASN45, ARG68, and LYS_76,

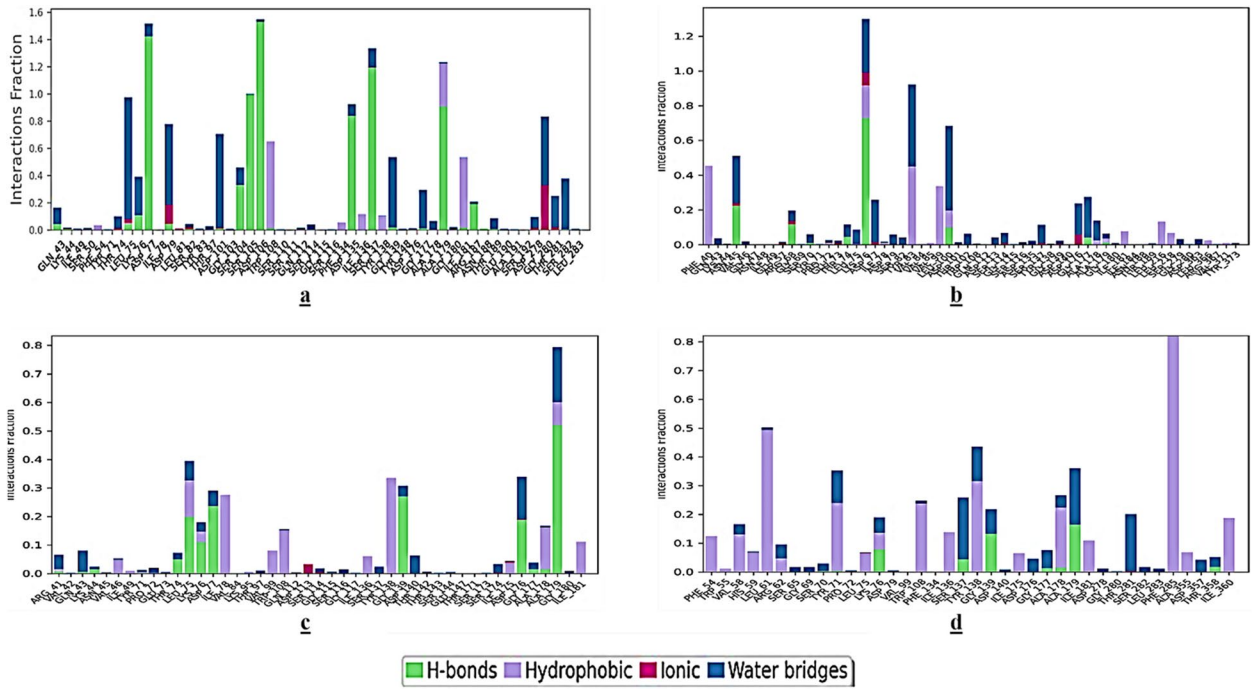

Fig. 13 The graphical illustration of different types of interactions occurred in docked complexes which majorly include hydrogen bonding and hydrophobic interactions (**a**): SAP-daidzin 4'-O-glucuronide complex; (**b**): SAP-fosmanogepix complex; (**c**): SAP-olorofim complex; (**d**): SAP-opelconazole complex

with interaction fractions nearing 1.0 or higher. This implied consistent hydrogen bonding throughout the simulation, contributing significantly to the binding stability. Similarly, the hydrophobic interactions were significantly observed for residues such as PHE40, TYR83, and VAL99 where they remained consistent throughout the simulation. These contacts, although less frequent than hydrogen bonds, indicated the importance of non-polar residue regions in maintaining ligand proximity and enhancing the stability. Likewise, several residues showed prominent interactions, such as LEU75, LYS76, ASP77, GLY139 and ALA179, indicating they were involved in significant binding with olorofim. The highest bar (Fig. 13 (c)), corresponding to ALA 180, suggested this residue might play a critical role in ligand binding or stabilization. Other significant residues like ILE 84 and ASP 174 also exhibited frequent and stable interactions. While, the residues such as LYS76, GLY139, and ALA179 exhibit notable hydrogen bonding, crucial for maintaining the opelconazole's conformation in the active site. Hydrogen bonding was observed to be essential for specific interactions which stabilized the ligand in its bound conformation. Furthermore, the residues such as PHE54, LEU61 ARG62, TYR71, PHE285 and ILE360 demonstrated significant hydrophobic contacts (Fig. 13 (d)), particularly with PHE285 showing the highest fraction (~ 0.8). These hydrophobic interactions indicated that opelconazole bound well within the non-polar pockets of the SAP protein, contributing to the stability of the complex.

Cumulative MMGBSA energy analysis

In this study, MM/GBSA binding energy calculations were performed using Desmond software, focusing on four ligands daidzin4'-O-glucuronide, fosmanogepix, olorofim, and opelconazole, in complex with the SAP protein. For this cumulative analysis, the last 20 ns of the molecular dynamics (MD) simulation, from 180 to 200 ns, were selected to represent the binding stability and affinity of each ligand. Daidzin4'-O-glucuronide (blue line) showed binding energies close to -65 kcal/mol, with some fluctuations, positioning it as a most stable complex. This result suggested that daidzin4'-O-glucuronide formed a relatively stable complex with SAP. Furthermore, the opelconazole (red line) also demonstrated the favorable binding energy, consistently around -70 kcal/mol. This stability indicates a strong interaction between SAP and opelconazole. Afterwards, olorofim (green line) exhibited binding energies around -50 kcal/mol, indicating moderate stability in its interaction with SAP. The increased fluctuations compared to the previously discussed two ligands may reflect conformational adjustments or weaker interactions. Moreover, the

fosmanogepix (orange line) displayed the least favorable binding energies, averaging around -40 kcal/mol. The larger fluctuations indicated a weaker affinity and stability in the SAP-fosmanogepix complex, suggesting that fosmanogepix may be less effective in binding SAP. All of these dynamic fluctuations in the energy levels can be observed in the Fig. 14.

Discussion

Many phytochemicals, especially plant flavonoids are found to be promising drugs against multiple harmful diseases and infections. These plant-based compounds are thus very much important as they possess significant therapeutic potential. Some of such scenarios in which their medicinal efficiency has been investigated include, different types of tumors and viral infections [35, 36]. Moreover, these compounds are also examined as antioxidants and anti-inflammatory agents in various research works [37–40]. Similarly, an *in-silico* approach was employed in one of the reported studies in which the therapeutic efficacy of certain natural compounds were examined against SARS-CoV-2. It was found that all of the incorporated plant compounds exhibited significant inhibition levels against the coronavirus [41].

On the basis of all such crucial findings and the reported therapeutic evidences of natural compounds, we have also employed such compounds from different plant sources in this particular study. The major targeted entity of this research was the putative candidapepsin protein of *C. lusitaniae* which is also known as Secreted Aspartyl Proteinase (SAP). Initially the amino acid sequence of the protein under investigation was retrieved from the UniProt database (https://www.uniprot.org/), in order to predict its three dimensional (3D) model. For this particular task, the trRosetta (https://yanglab.qd.sdu.edu.cn/trRosetta/), an online tool [42], was incorporated which utilizes the homology modeling approach to predict the 3D model of the given protein. A similar homology modelling approach has already been followed in a reported work in which certain plant flavonoids were tested as the inhibitors of plasmodium falciparum fatty acid biosynthesis (FAS-II Pathway) [43]. Furthermore, in the current perspective, the quality estimation of the modelled protein (SAP) was performed. In this regard, the Ramachandran Plot was constructed which was available on PROCHECK server (https://saves.mbi.ucla.edu/). It was found that the majority of the amino acid residues (92.7%) of the SAP model were allocated in the favorable region which signified that the predicted model was of good quality. One of the published research works has also employed the identical approach for the validation of predicted structure of nonstructural proteins of hepatitis C virus [44].

Afterwards, the molecular docking analysis was performed in which all of the selected phytochemicals were interacted with SAP to screen out the potent inhibitors on the basis of docking energy scores. For this purpose, the Molecular Operating Environment (MOE) was incorporated in which protein was initially prepared, prior to perform the docking analysis. Various parameters were considered in this perspective including the energy minimization of SAP structure by utilizing the energy minimization tool of MOE. The motive behind this action was to obtain an optimized conformation of the receptor protein and increase its stability during docking analysis. One of the published studies in which molecular docking and simulations were performed in order to study the antidiabetic agents that were derived from Hypoglycemic

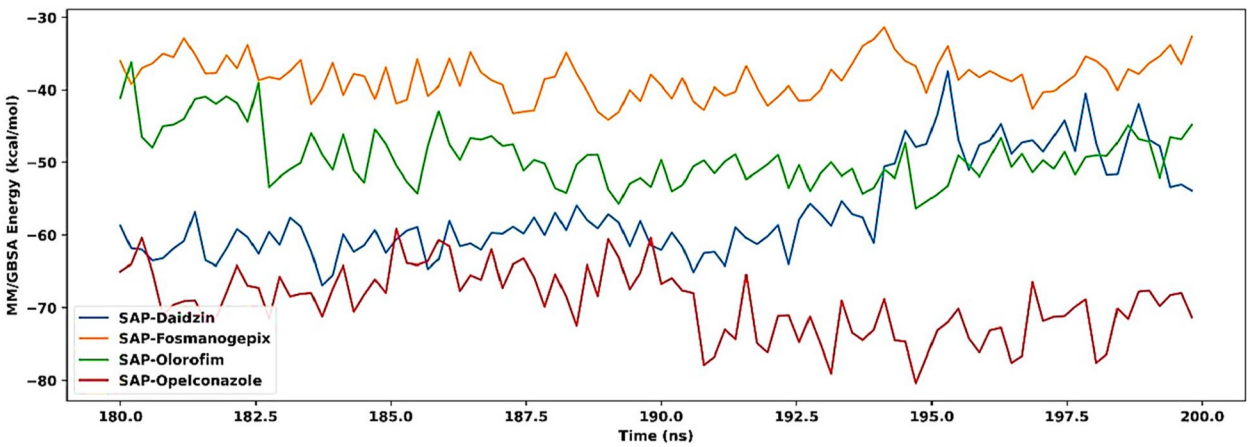

Fig. 14 The graphical representation of the MMGBSA energy analysis. Different colored peaks indicate respective complex which can be assessed by the scheme given in this fugure. It can be observed that daidzin4′-O-glucuronide and opelconazole exhibited comparatively better results in this regard, as compare to the rest ones

Polypeptide-P of *Momordica charantia*, has also reported to follow the similar energy minimization strategy [45].

Along with this, the ligands library of 35 natural compounds and 3 approved anti-fungal drugs was constructed locally in MOE. The corresponding chemical structures all the compounds were retrieved from ChEBI (https://www.ebi.ac.uk/chebi/) and PubChem (https://pubchem.ncbi.nlm.nih.gov/) databases. The selection of the incorporated phytocompounds was one of the crucial task to perform in this study. Hence, literature was conducted in which different reported studies were involved to short-list some of the effective antimicrobial and especially antifungal plant-based compounds [46–48]. Following the selection their respective structure data format (*.sdf*) files were retrieved from ChEBI accordingly, to prepare the ligands library. A similar method of ligands library preparation was followed in one of the reported research works in which the natural flavonoids, which showed an effective blockage of CD18 receptor of hepatocytes and thus efficiently inhibited the development of HCV infection. But, the phytochemicals which were selected for that specific research work, were retrieved from PubChem (https://pubchem.ncbi.nlm.nih.gov/) which is also a well-known hub of chemical compounds [49, 50], instead of ChEBI. However, the*.sdf* files of the control drugs were also retrieved from PubChem in this particular study. Subsequently, the molecular docking analysis of the receptor protein (SAP) was performed with the library of 38 ligands by selecting the Induced Fit Refinement (IFR) model and London dG scoring method which have also been reported by various other respective research investigations [51, 52].

Since, this molecular docking analysis was one of the key stages of the current study, therefore, the results of docking analysis were quite crucial as the final selection of potential compounds was based on these findings. Hence, after getting the docking results, a threshold value of -7.3 kcal/mol. was set to filter the best docked compounds. During this phase, only three compounds which included the opelconazole (-7.6 kcal/mol.) daidzin 4'0-glucuronide (-7.6 kcal/mol.) and naringin (-8.1 kcal/mol.), were shortlisted for the next and final round of selection. This first filtering phase was assisted by the scatter plot, constructed using the R language's '*read.xlsx*' and '*ggplot2*' packages. Further, the ADME analysis of these ligands was executed by utilizing an online tool, SwissADME (http://www.swissadme.ch/) which allows to study the drug properties of the given compounds. Some of the important factors were considered in this process including the pharmacokinetic properties, water solubility, CYP450 enzymes inhibition and Lipinski rule statuses. The crucial findings of this analysis suggested that only daidzin 4'0-glucuronide followed all of the required parameters. During the study of natural flavonoids as a potential inhibitors of Mitogen-activated protein kinase-3 (MAPK3), the researchers followed a homologous approach to investigate the pharmacokinetic properties of the flavonoids through SwissADME [53].

Moreover, to attain deeper insights of the docking interactions of finalized compound (daidzin 4'0-glucuronide) with the SAP, the ligPlot analysis was performed. This analysis provides with the schematic two dimensional (2D) representation of docking interactions of protein-ligand complexes. The results enabled us to visualize the intermolecular interactions including the hydrophobic and hydrophilic bonds between the protein (SAP) and ligand (daidzin 4'0-glucuronide). The significance of this analysis can be witnessed by the fact that many reported research works have utilized this method. For example, it was employed to comprehend the intermolecular bonding patterns of the docked complexes while examining the sulfonamed chalcone derivatives as alpha-glucosidase inhibitors [54]. Another reported study also employed the ligPlot analysis while studying the interactions of piperine with the cyclooxygenases [55].

Consequently, the molecular dynamics (MD) simulations of SAP-daidzin 4'0-glucuronide complex were executed. This analysis provides with the deeper insights regarding the structural stability and flexibility of the given docked complex. Pursuing the similar objective, we also performed the MD simulations of the SAP-daidzin 4'0-glucuronide docked complex to ensure whether the complex withstand different dynamic fluctuations. To perform this particular task, the Desmond software was incorporated. A major motive behind this analysis was to attain the comprehensive information about the docked complex that how it can flex, bend or changes its conformation as a result of various stimuli or conditions to attain a stable state. The findings of this study illustrated different maps including RSMD, RMSF, protein-ligand contacts which were quite significant in comprehending the dynamics of the complex. In this particular analysis, top three compounds from the selected library of phytocompounds, on the basis of binding affinities including daidzin 4'0-glucuronide along approved anti-fungal drugs were incorporated, in complex with SAP. The results suggested that SAP-daidzin 4'0-glucuronide docked complex possessed comparatively better structural stability and flexibility. During the *in-silico* designing of a potential ligand which could act as an inhibitor of mTOR pathway in breast cancer, molecular dynamics simulations of chromones and flavonoids were performed [56] to achieve the similar objectives. Whereas, the current strategic work was mainly aimed to not only identify and design a potential drug against candidapepsin protein of *C. lusitaniae* but also, to provide new directions for drug

development. However, the real-time efficacy of daidzin 4'0-glucuronide against SAP or candidapepsin protein of *C. lusitaniae* could only be attained upon clinical trials.

Conclusion

In this study, several phytochemicals were tested as potential drug candidates against secreted aspartyl proteinase of *C. lusitaniae*. Different computational approaches were involved in this study to achieve the core objective, including protein modelling, molecular docking analysis, ADME studies and molecular dynamics (MD) simulations. A total of 35 compounds from different plant sources and 3 of the approved anti-fungal drugs were subjected while, two phases for the selection of a final drug candidate were incorporated. During the first screening round, three compounds were filtered based upon the best docking scores. These compounds included opelconazole, daidzin 4'0-glucuronide and naringin with the docking scores of -7.6 kcal/mol., -7.6 kcal/mol. and -8.1 kcal/mol., respectively. Afterwards, the final scrutiny was enabled by the ADME investigation whose results identified daidzin 4'0-glucuronide to be the only compound which followed all of the required attributes of drug-likeness. In the end, the MD simulations were performed to comprehend the structural dynamics of the SAP- daidzin 4'0-glucuronide docked complex. For this purpose, the Desmond software was employed in order to gain a deeper understanding of the structural dynamism of the selected complexes. The results of MD simulations indicated SAP-daidzin 4'0-glucuronide complex to be a comparatively stable complex. Deeper understanding of the binding interactions was made possible by these simulations, which were crucial in examining the stability and conformational changes of the complex over time. This compound exhibited significantly better results in all of the incorporated analyses including molecular docking, MD simulations and most importantly, pharmacokinetics or drug-likeness analysis which none of the other compounds could completely followed. Such outcomes led to the conclusion that daidzin 4'0-glucuronide could be a promising inhibitor against SAP of *C. lusitaniae*. However, the actual therapeutic efficacy of daidzin 4'0-glucuronide against *C. lusitaniae* could only be achieved through clinical experimentations which indicates the limitation of this work.

Acknowledgements
The authors are thankful to the Deanship of Research and Graduate Studies, King Khalid University, Abha, Saudi Arabia, for supporting this work through the Large Research Group Project under Grant no. R.G.P2/509/45.

Clinical trial number
Not applicable (N/A).

Authors' contributions
RT and HN performed the analyses and wrote the manuscript. MFS designed the methodology, performed the software and proof-read the manuscript. UA and MD contributed in MD simulations analysis and validated the results. MFA performed the formal analysis. SA supervised the work. SOR managed the resources.

Funding
No funding was received for this research work.

Data availability
All relevant data are within the manuscript and its Supporting Information files.

Declarations

Ethics approval and consent to participate
Not applicable.

Consent for publication
Not applicable.

Competing interests
The authors declare no competing interests.

Received: 24 June 2024 Accepted: 23 December 2024
Published online: 06 January 2025

References

1. Sanchez V, et al. Epidemiology of nosocomial acquisition of Candida lusitaniae. J Clin Microbiol. 1992;30:3005–8.
2. Angiolella L, Rojas F, Giammarino A, Bellucci N & Giusiano G. Identification of Virulence Factors in Isolates of Candida haemulonii , Candida albicans and Clavispora lusitaniae with Low Susceptibility and Resistance to Fluconazole and Amphotericin B. 2024.
3. Wawrysiuk S, Rechberger T, Futyma K, Miotla P. Candida lusitaniae – a case report of an intraperitoneal infection. Menopausal Rev. 2018;17:94–6.
4. Sharma M & Chakrabarti A. Candidiasis and other emerging yeasts. Curr Fungal Infect Rep. 2023:15–24. https://doi.org/10.1007/s12281-023-00455-3.
5. Minari A, Hachem R, Raad I. Candida lusitaniae: a cause of breakthrough fungemia in cancer patients. Clin Infect Dis. 2001;32:186–90.
6. Atkinson BJ, Lewis RE, Kontoyiannis DP. Candida lusitaniae fungemia in cancer patients: risk factors for amphotericin B failure and outcome. Med Mycol. 2008;46:541–6.
7. de Melo Vieira AP, et al. Virulence factors of Candida spp. obtained from blood cultures of patients with candidemia attended at tertiary hospitals in Northeast Brazil. J Mycol Med. 2019;29:132–9.
8. Staniszewska M. Virulence Factors in Candida species. Curr Protein Pept Sci. 2020;21:313–23.
9. Pichová I, et al. Secreted aspartic proteases of Candida albicans, Candida tropicalis, Candida parapsilosis and Candida lusitaniae. Eur J Biochem. 2001;268:2669–77.
10. Shaw KJ. Fosmanogepix : a review of the first-in-class broad spectrum agent for the treatment of invasive fungal infections. 2020:1–21.
11. Hoenigl M, Sprute R, Egger M, Arastehfar A, Cornely OA. The antifungal pipeline : fosmanogepix , ibrexafungerp , olorofim. Drugs. 2021;81:1703–29.
12. Houšt J, Spížek J, Havlícek V. Antifungal drugs. Metabolites. 2020;10:106.
13. Pappas PG, et al. Clinical safety and efficacy of novel antifungal, fosmanogepix, for the treatment of candidaemia : results from a Phase 2 trial. J Antimicrob Chemother. 2023;78:2471–80.
14. Wiederhold NP. Review of the novel investigational antifungal olorofim. 2020.
15. Middleton, Jr., M.D., E. Biological properties of plant flavonoids: an overview. Int J Pharmacogn. 1996;34:344–348.

16. Dias MC, Pinto DCGA, Silva AMS. Plant flavonoids: chemical characteristics and biological activity. Molecules. 2021;26:5377.
17. Saleh M, Aboody A, Mickymaray S. Anti-Fungal Efficacy and Mechanisms of Flavonoids. 2020. https://doi.org/10.3390/antibiotics9020045.
18. Shen N, et al. Plant flavonoids: classification, distribution, biosynthesis, and antioxidant activity. Food Chem. 2022;383:132531.
19. Apweiler R, et al. UniProt: the universal protein knowledgebase. Nucleic Acids Res. 2004;32.
20. Du Z, et al. The trRosetta server for fast and accurate protein structure prediction. Nat Protoc. 2021;16:5634–51.
21. Anishchenko I, et al. Protein tertiary structure prediction and refinement using deep learning and Rosetta in CASP14. Proteins Struct Funct Bioinforma. 2021;89:1722–33.
22. International Tables for Crystallography. Int Tables Crystallogr. 2006:521–525. https://doi.org/10.1107/97809553602060000107.
23. Laskowski RA, MacArthur MW, Moss DS, Thornton JM. PROCHECK: a program to check the stereochemical quality of protein structures. J Appl Crystallogr. 1993;26:283–91.
24. Hollingsworth SA, Dror RO. Molecular dynamics simulation for all. Neuron. 2018;99:1129–43.
25. Saleh M, Aboody A & Mickymaray S. antibiotics Anti-Fungal E ffi cacy and Mechanisms of Flavonoids. 2020.
26. Tóth N, et al. Catechin potentiates the antifungal effect of miconazole in Candida glabrata. Folia Microbiol (Praha). 2023;68:835–42.
27. Glycolysis I, et al. Baicalein acts against Candida albicans by Targeting Eno1 and. 2022;10:1–16.
28. Degtyarenko K, et al. ChEBI: a database and ontology for chemical entities of biological interest. Nucleic Acids Res. 2007;36:D344–50.
29. Hastings J, et al. ChEBI in 2016: improved services and an expanding collection of metabolites. Nucleic Acids Res. 2016;44:D1214–9.
30. Daina A, Michielin O, Zoete V. SwissADME: A free web tool to evaluate pharmacokinetics, drug-likeness and medicinal chemistry friendliness of small molecules. Sci Rep. 2017;7:1–13.
31. Bakchi B, et al. An overview on applications of SwissADME web tool in the design and development of anticancer, antitubercular and antimicrobial agents: a medicinal chemist's perspective. J Mol Struct. 2022;1259:132712.
32. Riyadi PH, et al. SwissADME predictions of pharmacokinetics and drug-likeness properties of small molecules present in Spirulina platensis. IOP Conf Ser Earth Environ Sci. 2021;890:012021.
33. Laskowski RA, Swindells MB. LigPlot+: multiple ligand-protein interaction diagrams for drug discovery. J Chem Inf Model. 2011;51:2778–86.
34. Wallace AC, Laskowski RA, Thornton JM. LIGPLOT: a program to generate schematic diagrams of protein-ligand interactions. Protein Eng Des Sel. 1995;8:127–34.
35. Dehelean CA, et al. Drug Discovery and Alternative Therapy. 2021:1–29.
36. Mukhtar M, Arshad M, Ahmad M. Since January 2020 Elsevier has created a COVID-19 resource centre with free information in English and Mandarin on the novel coronavirus COVID- 19 . The COVID-19 resource centre is hosted on Elsevier Connect , the company ' s public news and information website . Elsevier hereby grants permission to make all its COVID-19-related research that is available on the COVID-19 resource centre - including this research content - immediately available in PubMed Central and other publicly funded repositories , such as the WHO COVID database with rights for unrestricted research re-use and analyses in any form or by any means with acknowledgement of the original source . These permissions are granted for free by Elsevier for as long as the COVID-19 resource centre. 2020. https://doi.org/10.1016/j.virusres.2007.09.008.
37. Jabeen M, et al. Exploring the antioxidant and anti-inflammatory potential of Wilckia maritima : in vitro and in silico investigations. 2023:1–16.
38. Faculty V. Anti-inflammatory and antioxidant properties of plant extracts. 2021;4:7–10.
39. Adegbola P, Aderibigbe I, Hammed W, Omotayo T. Antioxidant and anti-inflammatory medicinal plants have potential role in the treatment of cardiovascular disease : a review. 2017;7:19–32.
40. Li J, et al. Discovery of anti-inflammatory natural flavonoids: diverse scaffolds and promising leads for drug discovery. Eur J Med Chem. 2023;260:115791.
41. Kashyap P, et al. In silico evaluation of natural flavonoids as a potential inhibitor of coronavirus disease. Molecules. 2022;27:6374.
42. Su H, et al. Improved protein structure prediction using a new multi-scale network and homologous templates. Adv Sci. 2021;8.
43. Pandey A, Shyamal SS, Shrivastava R, Ekka S, Mali SN. Inhibition of Plasmodium falciparum Fatty Acid Biosynthesis (FAS-II Pathway) by natural flavonoids: a computer-aided drug designing approach. Chem Africa. 2022;5:1469–91.
44. Sajitha Lulu S, Thabitha A, Vino S, Mohana Priya A, Rout M. Naringenin and quercetin – potential anti-HCV agents for NS2 protease targets. Nat Prod Res. 2016;30:464–8.
45. Arif R, et al. Molecular Docking and Simulation Studies of Antidiabetic Agents Devised from Hypoglycemic Polypeptide-P of Momordica charantia. Biomed Res Int. 2021;2021:1–15.
46. Shinde RB, Raut JS, Chauhan NM, Karuppayil SM. Original article Chloroquine sensitizes biofilms of Candida albicans to antifungal azoles. Brazilian J Infect Dis. 2013;17:395–400.
47. Lee, W. & Lee, D. G. An Antifungal mechanism of curcumin lies in membrane-targeted action within Candida albicans. 780–785. https://doi.org/10.1002/iub.1326.
48. Panagoda GJ, Yau J, Samaranayake LP. Antifungal Activity of Black Tea Polyphenols (Catechins and Theaflavins) against Candida Species. 2009:189–196. https://doi.org/10.1159/000216836.
49. Dey D, et al. Natural flavonoids effectively block the CD81 receptor of hepatocytes and inhibit HCV infection: a computational drug development approach. Mol Divers. 2023;27:1309–22.
50. Kim S, et al. PubChem substance and compound databases. Nucleic Acids Res. 2016;44:D1202–13.
51. Liu M-M, et al. Discovery of flavonoid derivatives as anti-HCV agents via pharmacophore search combining molecular docking strategy. Eur J Med Chem. 2012;52:33–43.
52. Aminu KS, Uzairu A, Abechi SE, Shallangwa GA, Umar AB. Activity prediction, structure-based drug design, molecular docking, and pharmacokinetic studies of 1,4-dihydropyridines derivatives as a-amylase inhibitors. J Taibah Univ Med Sci. 2024;19:270–86.
53. Taherkhani A, Khodadadi P, Samie L, Azadian Z, Bayat Z. Flavonoids as strong inhibitors of MAPK3: a computational drug discovery approach. Int J Anal Chem. 2023;2023:1–16.
54. Bharatham K, Bharatham N, Park KH, Lee KW. Binding mode analyses and pharmacophore model development for sulfonamide chalcone derivatives, a new class of a-glucosidase inhibitors. J Mol Graph Model. 2008;26:1202–12.
55. Karunakar P, et al. In silico docking analysis of piperine with cyclooxygenases. J Biochem Technol. 2012;3:S122-127.
56. Sharma V, Panwar A, Sharma AK. Molecular dynamic simulation study on chromones and flavonoids for the in silico designing of a potential ligand inhibiting mTOR pathway in breast cancer. Curr Pharmacol Reports. 2020;6:373–9.

Publisher's Note